41st ISYA Lecturer: *Gustavo Bruzual, IRyA, UNAM; Campus Morelia, México*

Topic: *GALAXIES (6 lectures)*

Description: An overview of the basic properties of galaxies due to the distribution, kinematics, dynamics, relevance, and evolution of their different stellar populations. A view of the basic properties and processes in the distant universe as revealed by galaxies of all types discovered so far.

Syllabus:

Lecture 1: **The Milky Way as a galaxy**
- The structure of the Galaxy
- The galactic disk
- The galactic bulge
- The galactic halo
- The galactic center
- Velocity of the sun
- Rotation curve of the Galaxy
- Stellar populations in the Galaxy

Lecture 2: **The world of galaxies (1)**
- Morphological classification. The Hubble Sequence
- Other types of galaxies
- Elliptical galaxies
- Spiral galaxies
- Galaxies in the local group
- Scaling relations

Lecture 3: **The world of galaxies (2)**
- The extragalactic distance scale
- The luminosity function of galaxies
- Black holes in the centers of galaxies
- Galaxies as gravitational lenses
- Stellar population synthesis
- Spectral evolution of galaxies
- Chemical evolution of galaxies

Lecture 4: **Clusters and groups of galaxies**
- The local group
- Galaxies in clusters and groups
- Morphological classification of clusters
- Spatial distribution of galaxies in clusters
- Luminosity function of cluster galaxies
- Clusters of galaxies as gravitational lenses
- Evolution of clusters

Lecture 5: **Galaxies at high redshift (1)**
- Lyman-break galaxies
- Starburst galaxies
- Extremely red objects
- Sub-millimeter sources
- Damped Lyman-alpha systems
- Lyman-alpha blobs
- Gamma-ray bursts

Lecture 6: **Galaxies at high redshift (2)**
- Background radiation
- Re-ionization of the universe
- Cosmic star formation history
- Galaxy formation and evolution

Requirements: Video projector in the class room

Bibliography:

- Schneider, *Extragalactic astronomy and cosmology*
- Sparke & Gallager, *Galaxies in the Universe*
- Mo, van den Bosch & White, Galaxy formation and evolution (selected chapters)

Lecture I: The Milky Way as a Galaxy

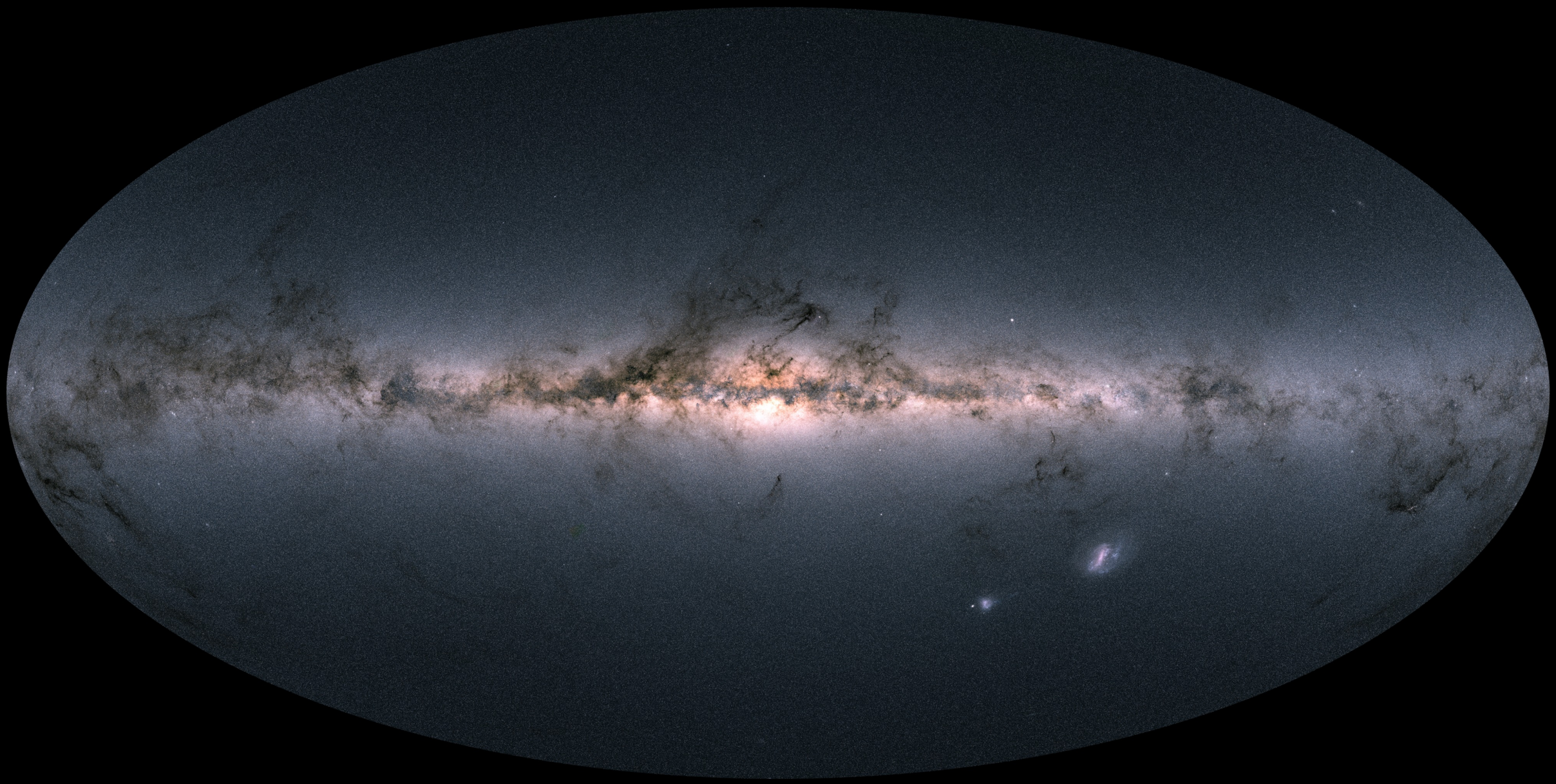

G. Bruzual, IRyA, UNAM, Morelia, México

Gaia view of the Milky Way Galaxy (as of April 2018 DR2)

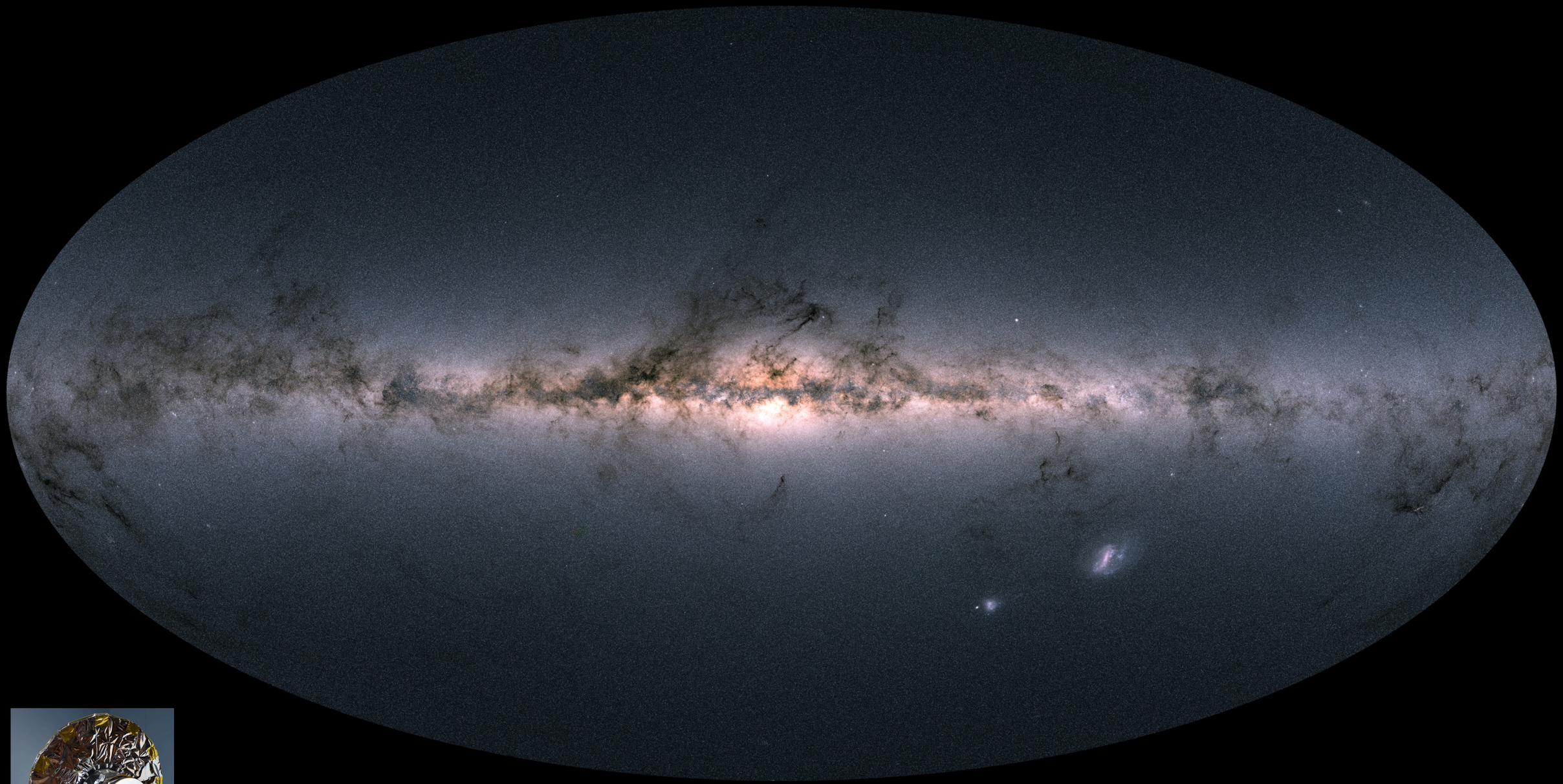

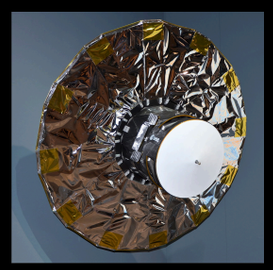

Gaia Satellite

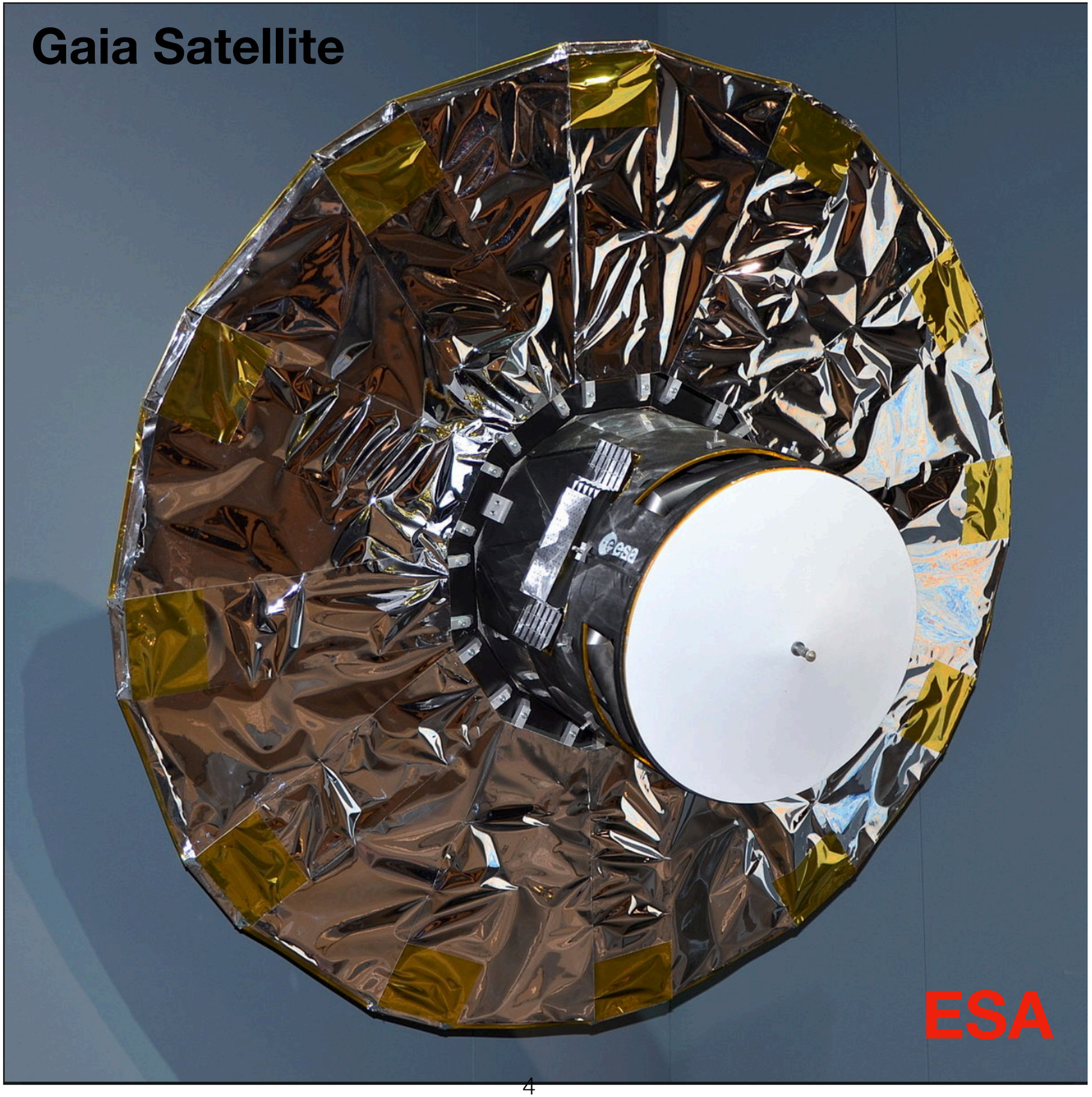

Trigonometric Parallax

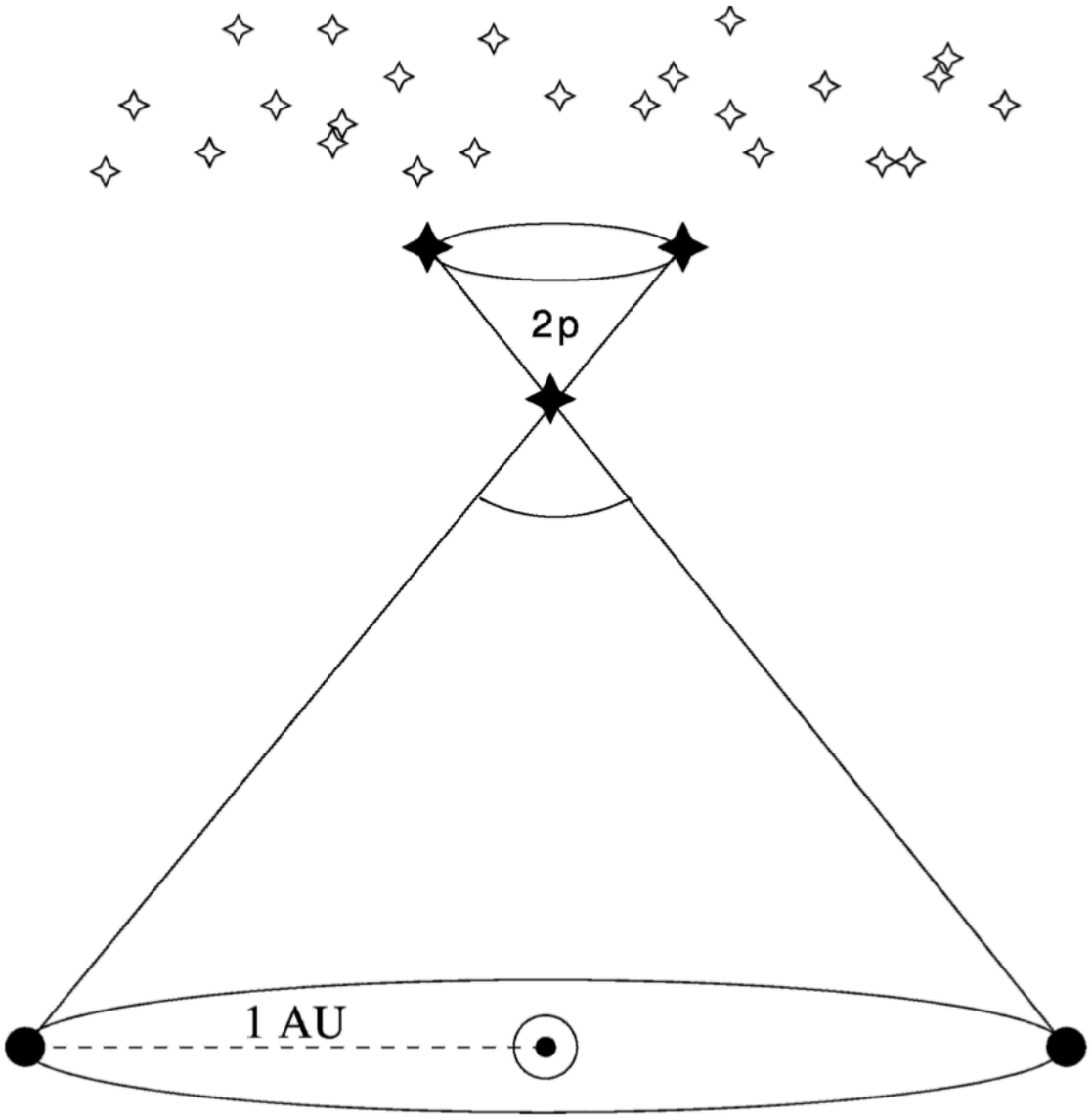

Fig. 2.3. Illustration of the parallax effect: in the course of the Earth's orbit around the Sun the apparent positions of nearby stars on the sky seem to change relative to those of very distant background sources

The distance corresponding to a measured parallax is then calculated as

$$D = \left(\frac{p}{1''}\right)^{-1} \text{pc} \quad . \tag{2.4}$$

$$\frac{r}{D} = \tan p \approx p \ ,$$

$$1 \text{ pc} = 206\,265 \text{ AU} = 3.086 \times 10^{18} \text{ cm} \quad .$$

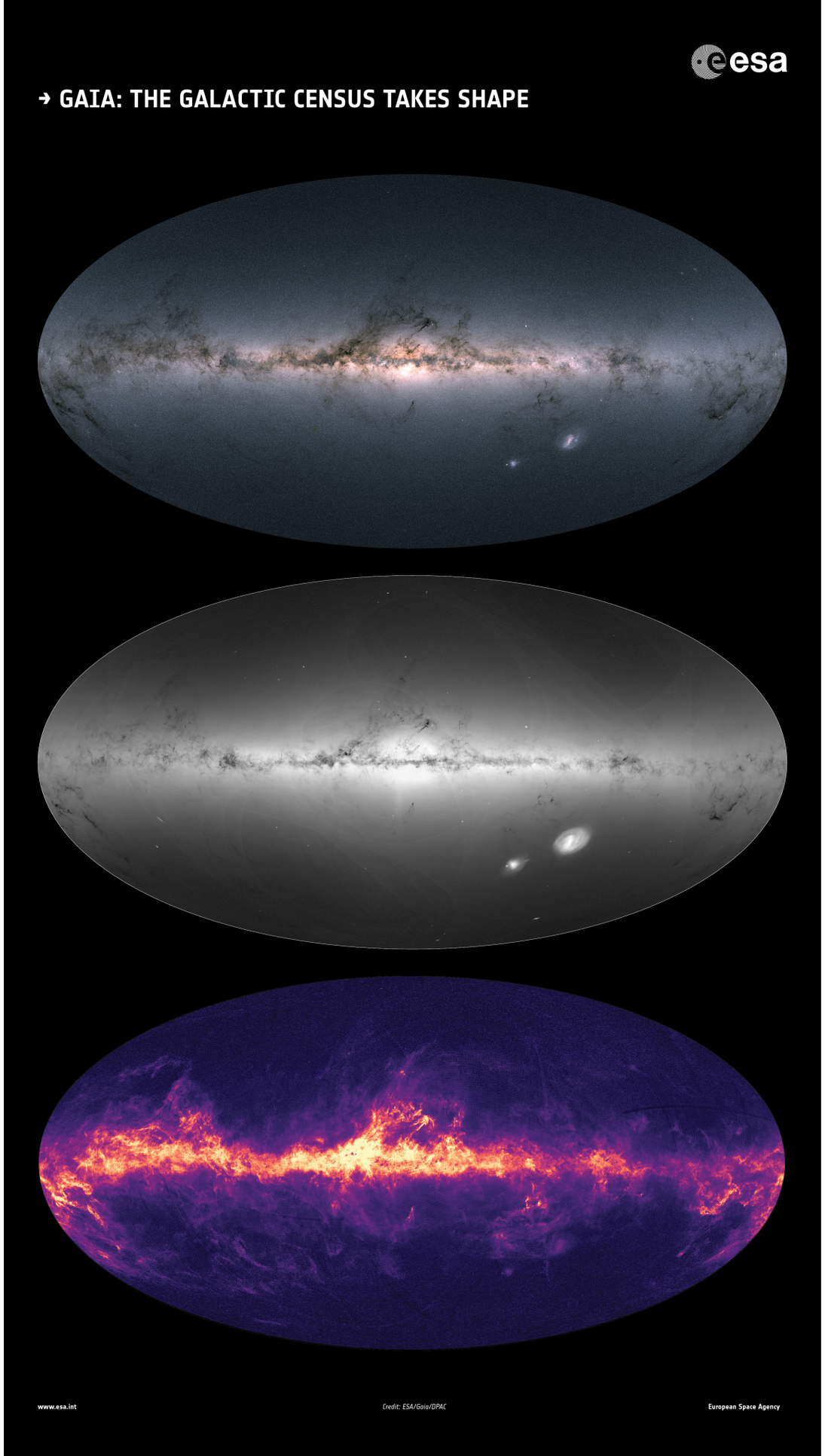

Gaia DR2: high precision measurements for

$$1.7 \times 10^9 \text{ stars}$$

<— Total brightness and color of the stars

<— Total density of the stars

<— Interstellar dust that fills the galaxy

Views of the Milky Way

Our galaxy

Seen protected on the sky

We live in the Milky Way's disk

How many of you have seen the MW?

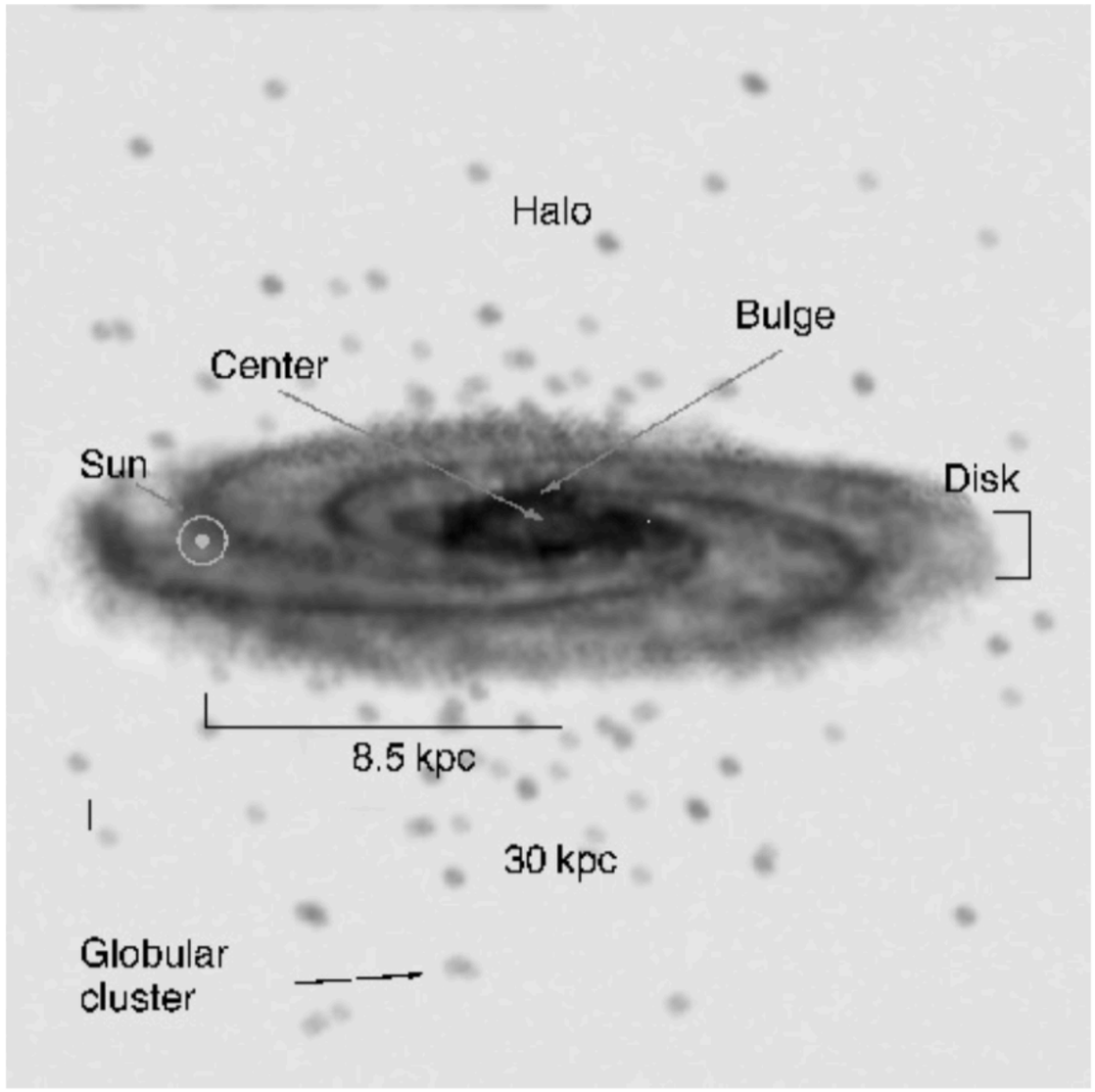

Fig. 1.3. Schematic structure of the Milky Way consisting of the disk, the central bulge with the Galactic center, and the spherical halo in which most of the globular clusters are located. The Sun orbits around the Galactic center at a distance of about 8 kpc

Schematic View of the Galaxy

Disk (youngest stars)

Bulge

Halo (oldest stars)

Spiral Arms

Bar

A New Look at a Milky Way Analogue

The MW also has a bar

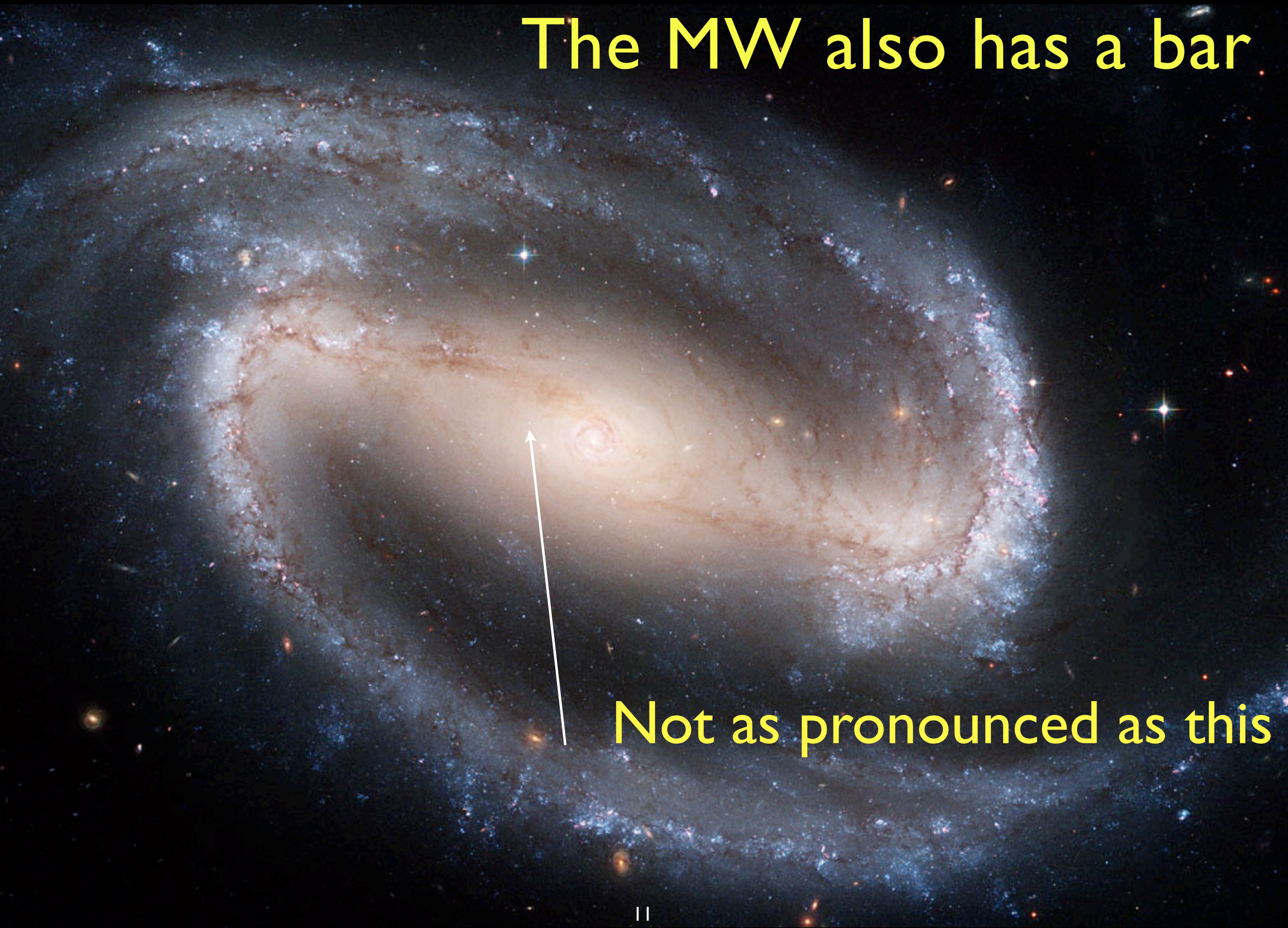

Not as pronounced as this

Structure of the Galaxy

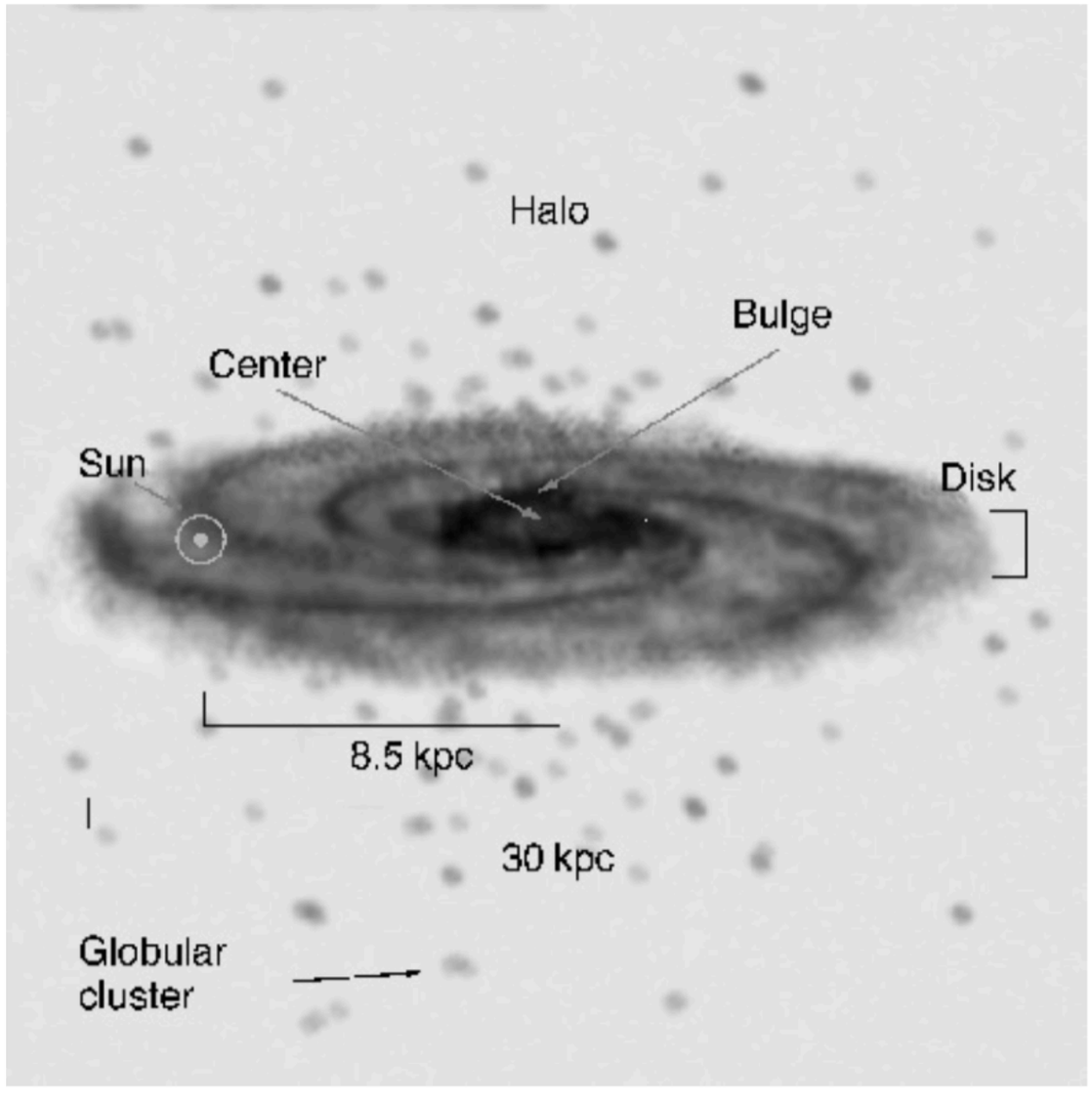

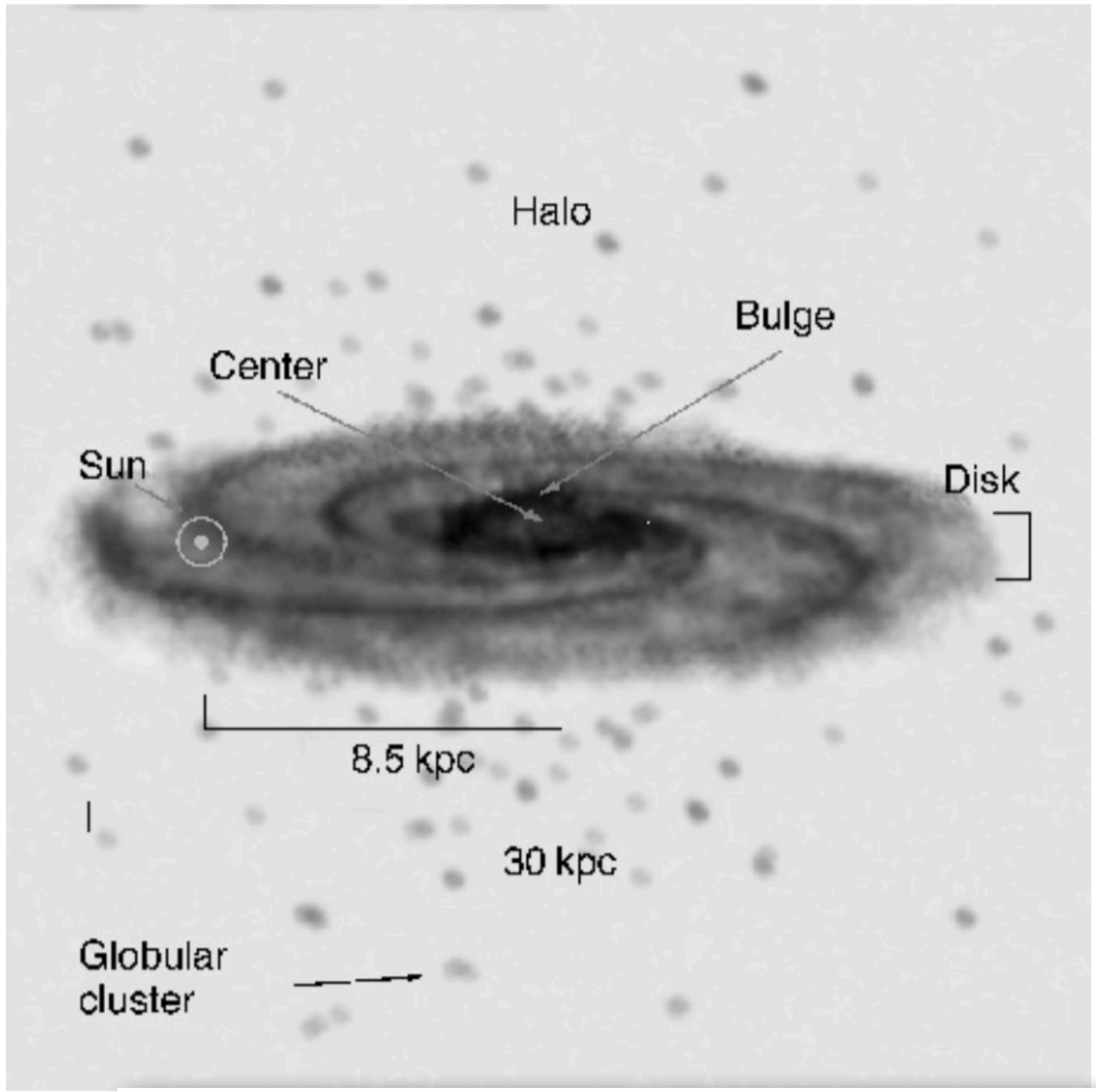

$$n(z) \propto \exp\left(-\frac{|z|}{h}\right) ,$$

$$\sigma_i^2 = \left\langle (v_i - \langle v_i \rangle)^2 \right\rangle = \left\langle v_i^2 - \langle v_i \rangle^2 \right\rangle$$
$$= n^{-1} \int_{\mathbb{R}^3} \mathrm{d}^3 v \; f(\boldsymbol{v}) \; \left(v_i^2 - \langle v_i \rangle^2\right) .$$

$$\boxed{n(R,z) = n_0 \left(\mathrm{e}^{-|z|/h_{\mathrm{thin}}} + 0.02\mathrm{e}^{-|z|/h_{\mathrm{thick}}}\right) \mathrm{e}^{-R/h_R}}$$

$$\boxed{L(R,z) = \frac{L_0 \mathrm{e}^{-R/h_R}}{\cosh^2(z/h_z)}} ,$$

with $h_z = 2h_{\mathrm{thin}}$ and $L_0 \approx 0.05 L_\odot/\mathrm{pc}^3$.

Table 2.1. Parameters and characteristic values for the components of the Milky Way. The scale-height denotes the distance from the Galactic plane at which the density has decreased to 1/e of its central value. σ_z is the velocity dispersion in the direction perpendicular to the disk

	Neutral gas	Thin disk	Thick disk	bulge	Stellar halo	Dm halo
M ($10^{10}\mathrm{M}_\odot$)	0.5	6	0.2 to 0.4	1	0.1	55
L_B ($10^{10}\mathrm{L}_\odot$)	–	1.8	0.02	0.3	0.1	0
M/L_B ($\mathrm{M}_\odot/\mathrm{L}_\odot$)	–	3	–	3	~ 1	–
diam. (kpc)	50	50	50	2	100	> 200
form	$\mathrm{e}^{-h_z/z}$	$\mathrm{e}^{-h_z/z}$	$\mathrm{e}^{-h_z/z}$	bar?	$r^{-3.5}$	$(a^2+r^2)^{-1}$
scale-height (kpc)	0.13	0.325	1.5	0.4	3	2.8
σ_z ($\mathrm{km\,s}^{-1}$)	7	20	40	120	100	–
[Fe/H]	> 0.1	-0.5 to $+0.3$	-1.6 to -0.4	-1 to $+1$	-4.5 to -0.5	–

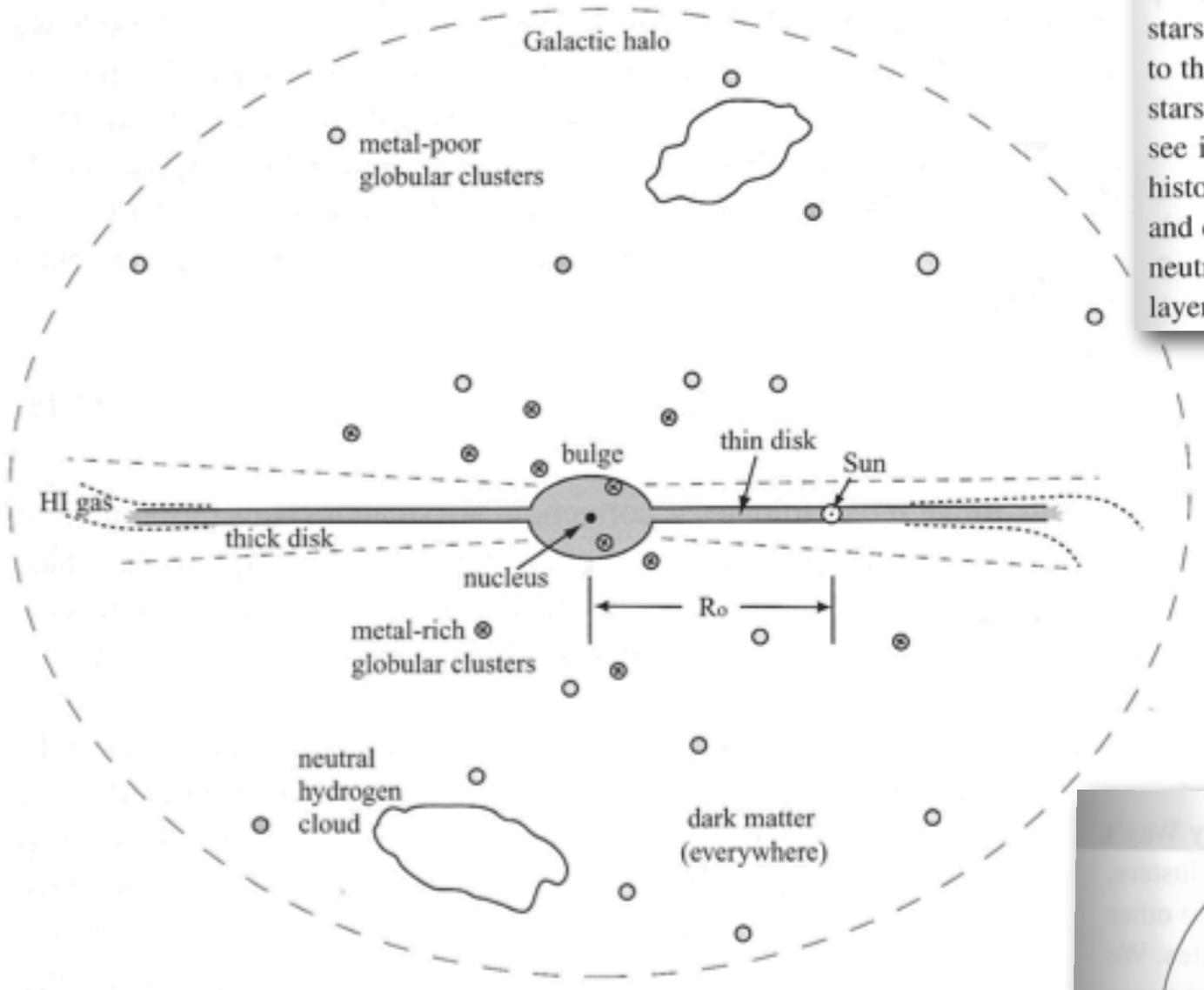

Fig. 1.8. A schematic side view of the Milky Way.

The *thin disk* contains 95% of the disk stars, and all of the young massive stars. Its *scale height*, the distance we must move in the direction perpendicular to the disk to see the density fall by a factor of e, is 300–400 pc. The rest of the stars form the *thick disk*, which has a larger scale height of about 1 kpc. We will see in Chapter 2 that stars of the thick disk were made earlier in the Galaxy's history than those of the thin disk, and they are poorer in heavy elements. The gas and dust of the disk lie in a very thin layer; near the Sun's position, most of the neutral hydrogen gas is within 100 pc of the midplane. The thickness of the gas layer increases roughly in proportion to the distance from the Galactic center.

Milky Way

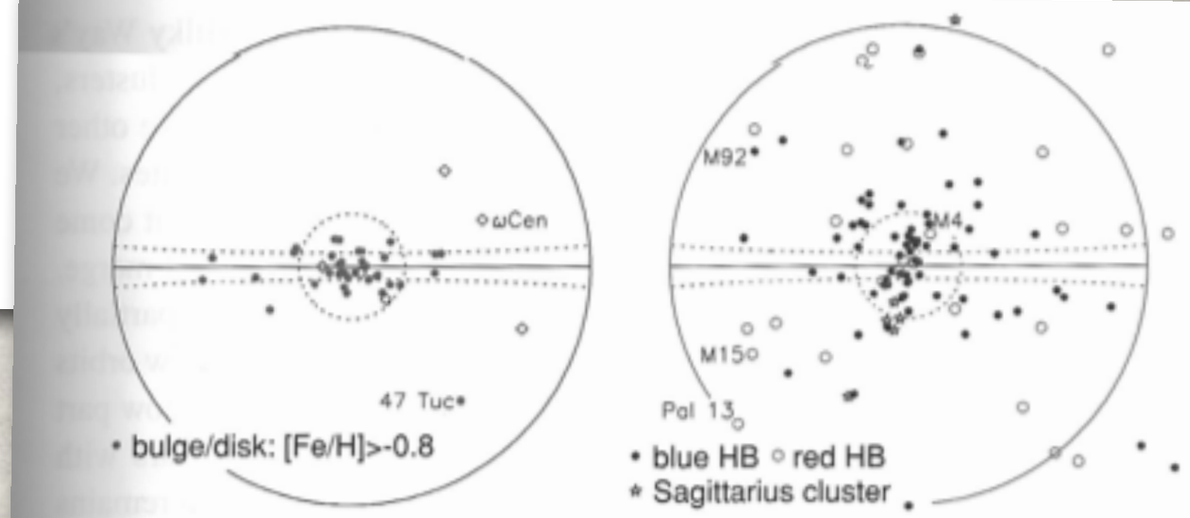

Fig. 2.15. Left, positions on the sky of the Milky Way's metal-rich 'disk' globular clusters (filled dots), and unusual objects, perhaps remnants of disrupted dwarf galaxies (open diamonds). Right, metal-poor clusters with [Fe/H] < -0.8. Those of the Sagittarius dwarf (stars) fall in a great circle on the sky. Clusters with a blue horizontal branch (filled dots) are more concentrated to the center than are those with a red horizontal branch (open circles). Circles mark 20° and 90° from the direction to the Galactic center; the solid line is the Galactic equator. Between the dashed lines at $b = \pm 5°$, clusters may easily hide in the dusty disk – D. Mackey.

Molecular Clouds

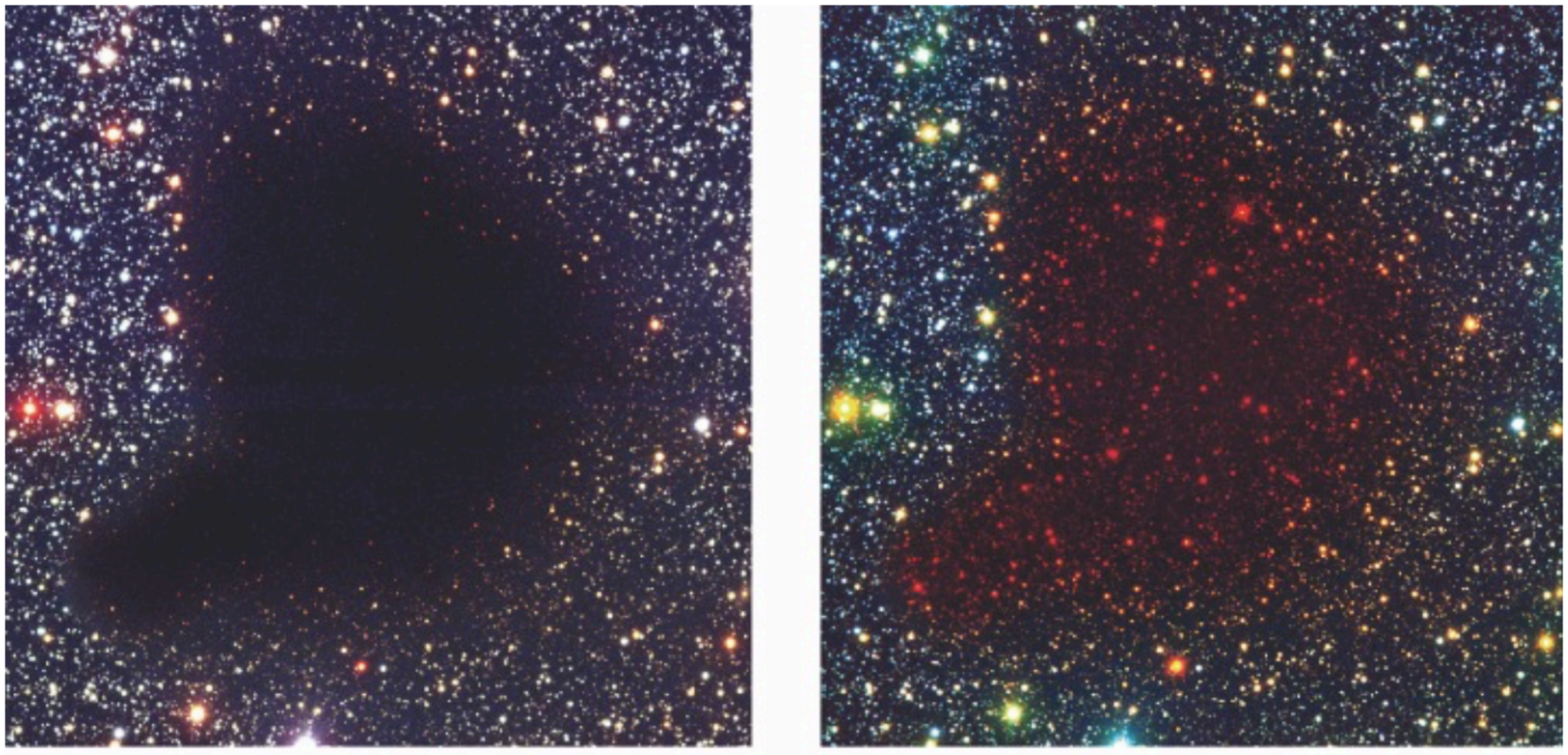

Fig. 2.7. These images of the molecular cloud Barnard 68 show the effects of extinction and reddening: the left image is a composite of exposures in the filters B, V, and I. At the center of the cloud essentially all the light from the background stars is absorbed. Near the edge it is dimmed and visibly shifted to the red. In the right-hand image observations in the filters B, I, and K have been combined (red is assigned here to the near-infrared K-band filter); we can clearly see that the cloud is more transparent at longer wavelengths

Extinction Laws

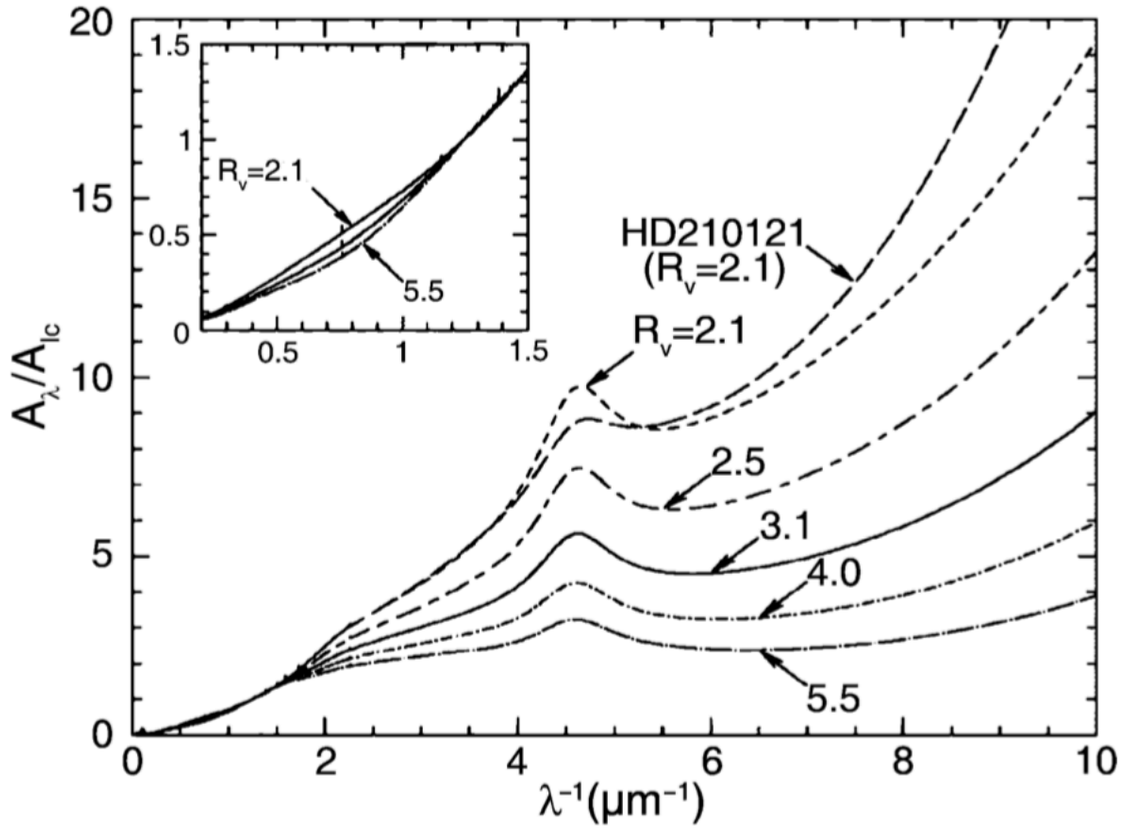

Fig. 2.6. Wavelength dependence of the extinction coefficient A_ν, normalized to the extinction coefficient A_I at $\lambda = 9000$ Å. Different kinds of clouds, characterized by the value of R_V, i.e., by the reddening law, are shown. On the x-axis we have plotted the inverse wavelength, so that the frequency increases to the right. The solid line specifies the mean Galactic extinction curve. The extinction coefficient, as determined from the observation of an individual star, is also shown; clearly the observed law deviates from the model in some details. The figure insert shows a detailed plot at relatively large wavelengths in the NIR range of the spectrum; at these wavelengths the extinction depends only weakly on the value of R_V

The Galactic Center

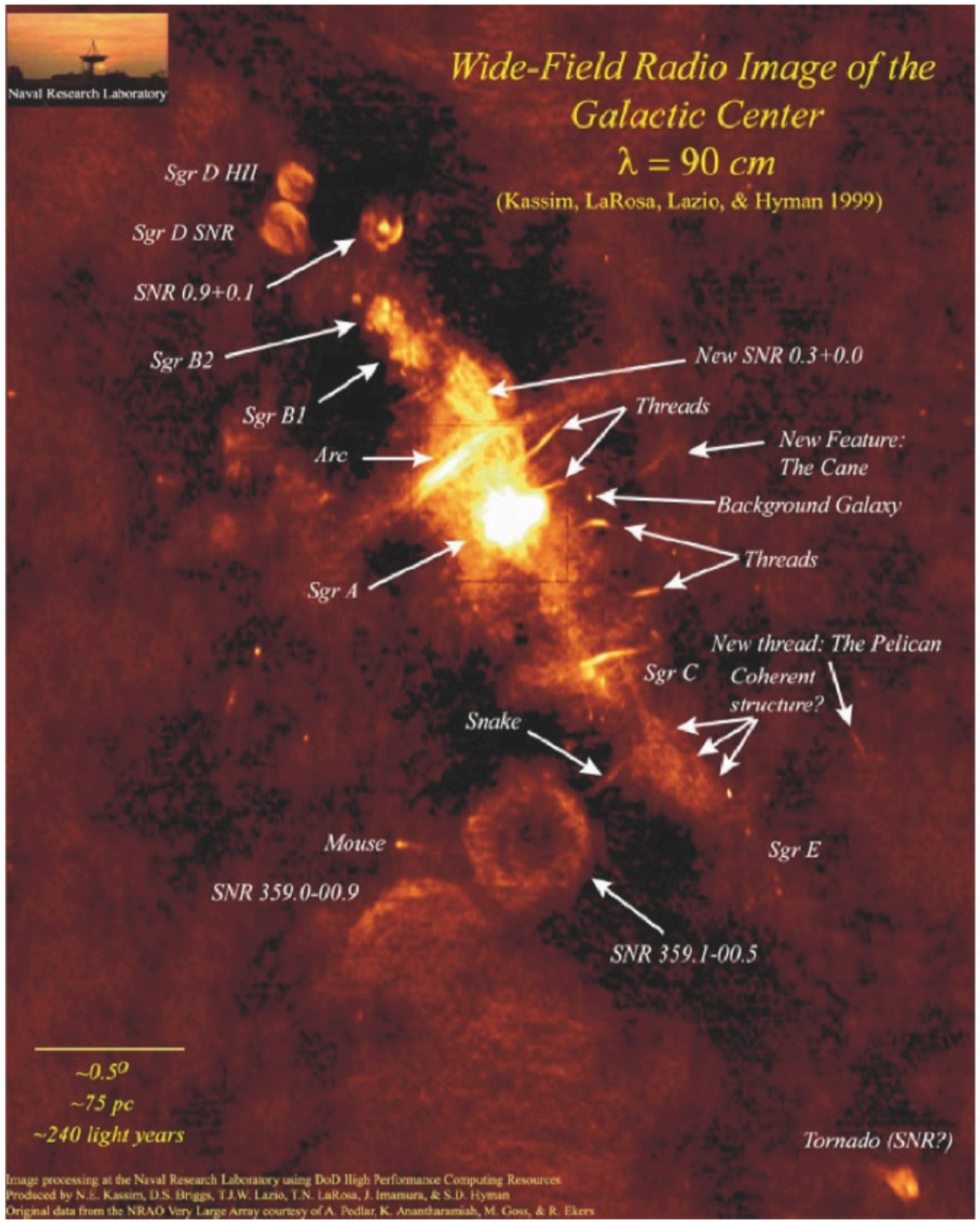

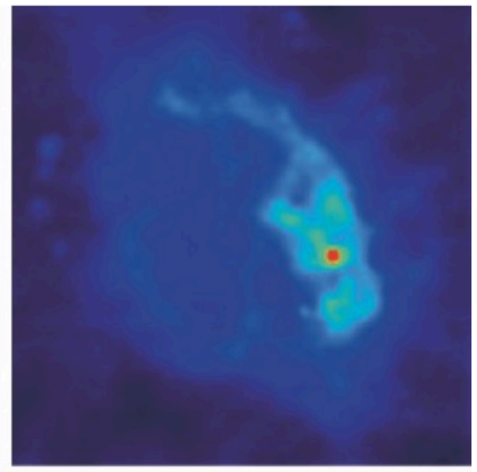

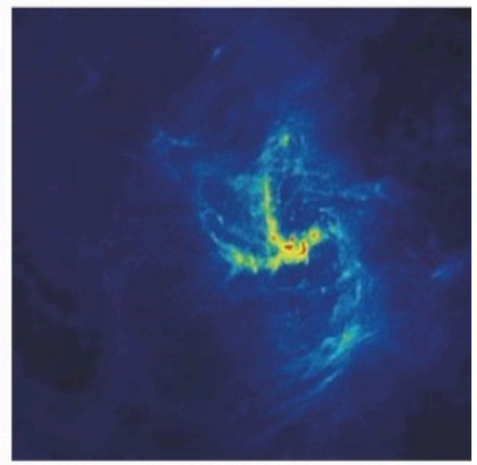

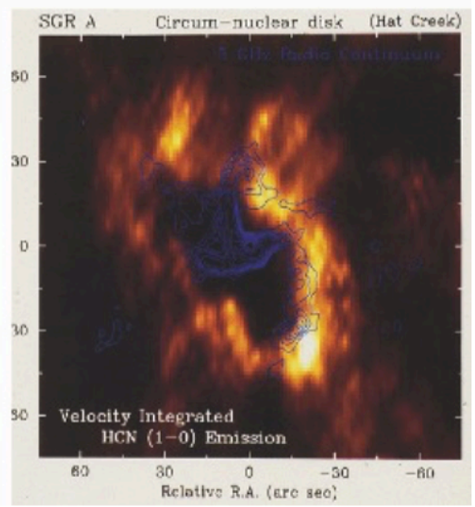

Fig. 2.34. Left: A VLA wide-field image of the region around the Galactic center, with a large number of sources identified. Upper right: a 20 cm continuum VLA image of Sgr A East, where the red dot marks Sgr A*. Center right: Sgr A West, as seen in a 6-cm continuum VLA image. Lower right: the circumnuclear ring in HCN line emission

The Galactic Center

Fig. 2.35. Mosaic of X-ray images of the Galactic center, taken by the Chandra satellite. The image covers an area of about 130 pc × 300 pc ($48' \times 120'$). The actual GC, in which a supermassive black hole is suspected to reside, is located in the white region near the center of the image. Furthermore, on this image hundreds of white dwarfs, neutron stars, and black holes are visible that radiate in the X-ray regime due to accretion phenomena (accreting X-ray binaries). Colors code the photon energy, from low energy (red) to high energy (blue). The diffuse emission, predominantly red in this image, originates in diffuse hot gas with a temperature of about $T \sim 10^7$ K

The Galactic Center

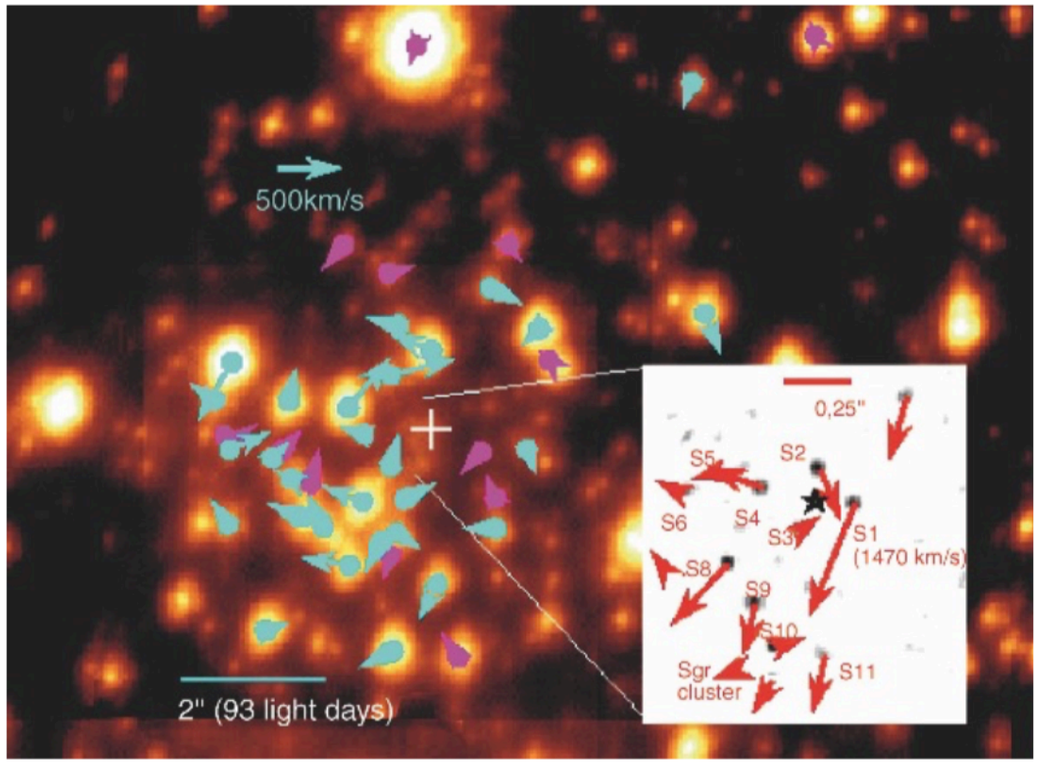

Fig. 2.36. Proper motions of stars in the central region of the GC. The differently colored arrows denote different types of stars. The small image shows the proper motions in the Sgr A* star cluster within half an arcsecond from Sgr A*; the fastest star (S1) has a proper motion of ~ 1500 km/s (from Genzel, 2000, astro-ph/0008119

The kinematics of stars in the central star cluster of the Galaxy shows that our Milky Way contains a mass concentration in which $\sim 3 \times 10^6 M_\odot$ are concentrated within a region smaller than 0.01 pc. This is most probably a black hole in the center of our Galaxy at the position of the compact radio source Sgr A*.

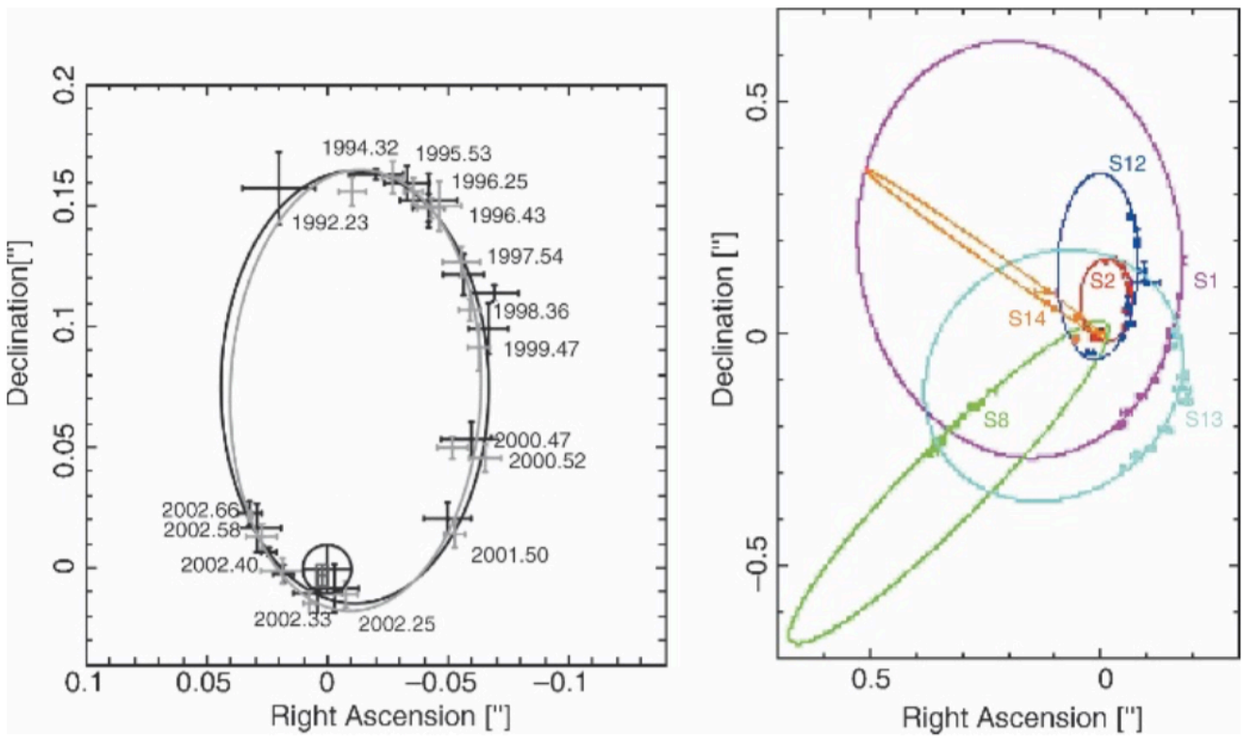

Fig. 2.37. At left, the orbit of the star S2 around Sgr A* is shown as determined by two different observing campaigns. The position of Sgr A* is indicated by the black circled cross. The individual points along the orbit are identified by the epoch of the observation. The right-hand image shows the orbits of some other stars for which accelerations have already been measured

Rotation of the Galaxy

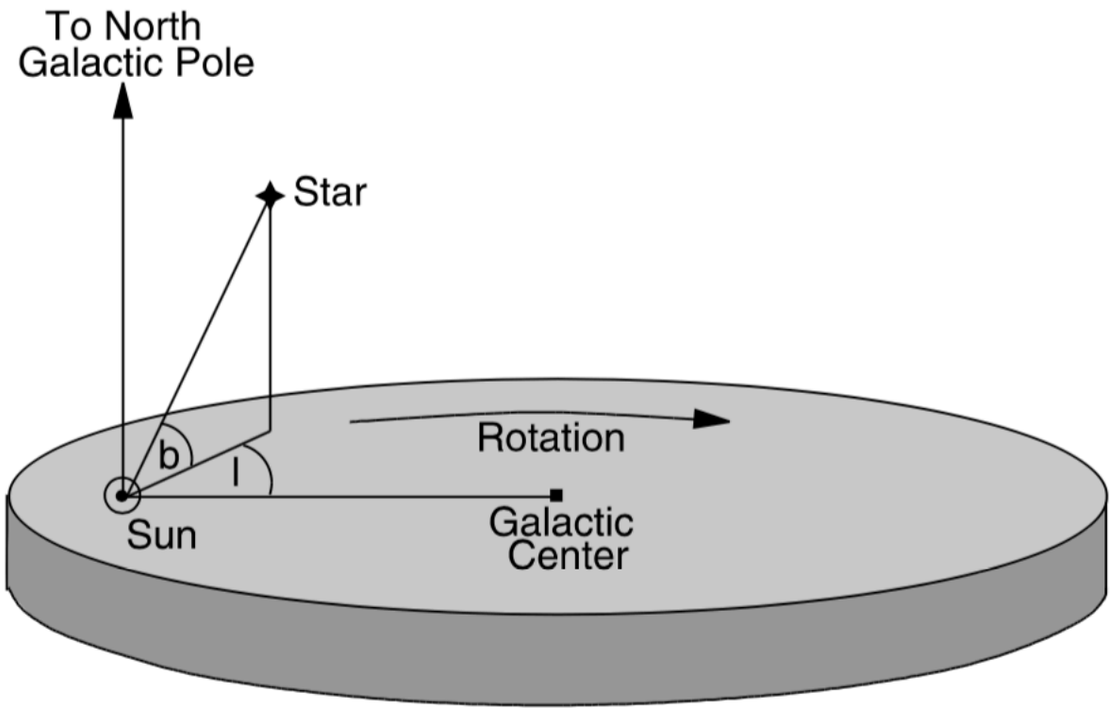

Fig. 2.2. The Sun is at the origin of the Galactic coordinate system. The directions to the Galactic center and to the North Galactic Pole (NGP) are indicated and are located at $\ell = 0°$ and $b = 0°$, and at $b = 90°$, respectively

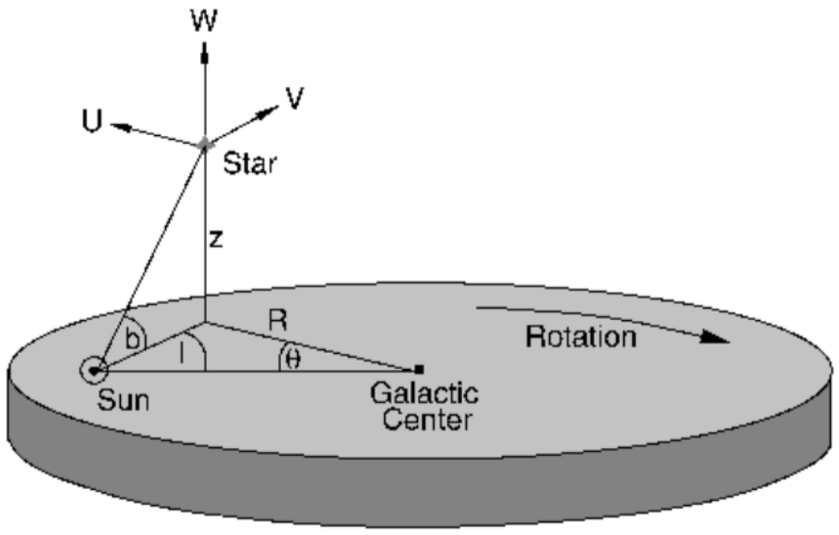

Fig. 2.13. Cylindrical coordinate system (R, θ, z) with the Galactic center at its origin. Note that θ increases in the clockwise direction if the disk is viewed from above. The corresponding velocity components (U, V, W) of a star are indicated

Galactic Rotation

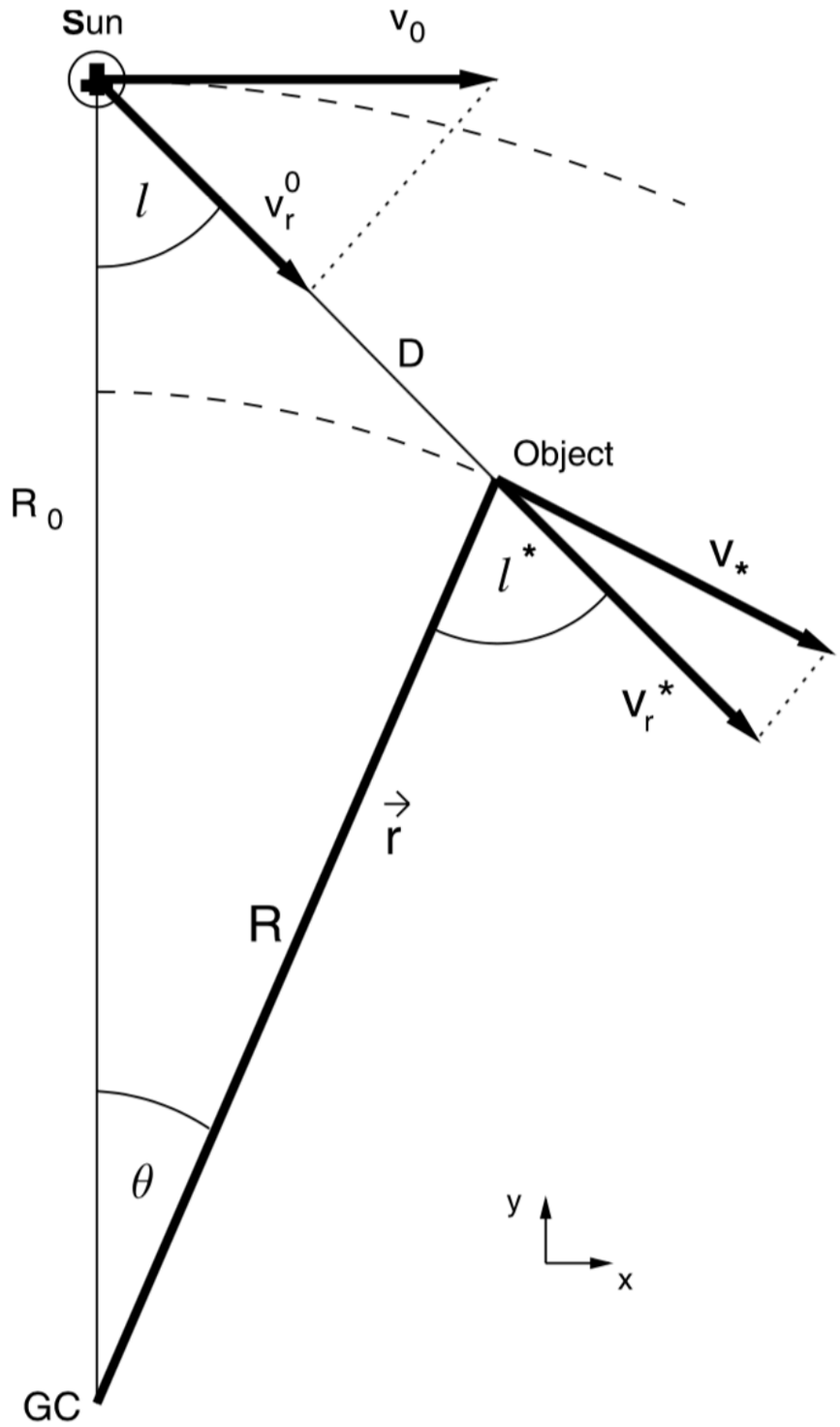

Fig. 2.16. Geometric derivation of the formalism of differential rotation:

$$v_\mathrm{r} = v_\mathrm{r}^* - v_\mathrm{r}^\odot = v_* \sin\ell^* - v_\odot \sin\ell \,,$$
$$v_\mathrm{t} = v_\mathrm{t}^* - v_\mathrm{t}^\odot = v_* \cos\ell^* - v_\odot \cos\ell \,.$$

With the angular velocity defined as

$$\Omega(R) = \frac{V(R)}{R} \,, \tag{2.56}$$

we obtain for the relative velocity

$$\Delta V = \begin{pmatrix} R_0(\Omega - \Omega_0) - \Omega\, D\, \cos\ell \\ -D\,\Omega\, \sin\ell \end{pmatrix} \,,$$

where $\Omega_0 = V_0/R_0$ is the angular velocity of the Sun. The radial and tangential velocities of this relative motion then follow by projection of ΔV along the direction parallel or perpendicular, respectively, to the separation vector,

$$\boxed{v_\mathrm{r} = \Delta V \cdot \begin{pmatrix} \sin\ell \\ -\cos\ell \end{pmatrix} = (\Omega - \Omega_0) R_0 \sin\ell} \,, \tag{2.57}$$

$$\boxed{v_\mathrm{t} = \Delta V \cdot \begin{pmatrix} \cos\ell \\ \sin\ell \end{pmatrix} = (\Omega - \Omega_0) R_0 \cos\ell - \Omega\, D} \,. \tag{2.58}$$

A purely geometric derivation of these relations is given in Fig. 2.16.

For $|R - R_0| \ll R_0$ it follows that $R_0 - R \approx D\cos\ell$; if we insert this into (2.60) and (2.61) we get

$$\boxed{v_\mathrm{r} \approx A\,D\,\sin 2\ell \;, \quad v_\mathrm{t} \approx A\,D\,\cos 2\ell + B\,D} \;, \tag{2.62}$$

where A and B are the *Oort constants*

$$\boxed{\begin{aligned} A &:= -\frac{1}{2}\left[\left(\frac{\mathrm{d}V}{\mathrm{d}R}\right)_{|R_0} - \frac{V_0}{R_0}\right] , \\ B &:= -\frac{1}{2}\left[\left(\frac{\mathrm{d}V}{\mathrm{d}R}\right)_{|R_0} + \frac{V_0}{R_0}\right] \end{aligned}} \;. \tag{2.63}$$

The radial and tangential velocity fields relative to the Sun show a sine curve with period π, where v_t and v_r are phase-shifted by $\pi/4$. This behavior of the velocity field in the Solar neighborhood is indeed observed (see Fig. 2.17). By fitting the data for $v_\mathrm{r}(\ell)$ and $v_\mathrm{t}(\ell)$ for stars of equal distance D one can determine A and B, and thus

$$\boxed{\Omega_0 = \frac{V_0}{R_0} = A - B, \quad \left(\frac{\mathrm{d}V}{\mathrm{d}R}\right)_{|R_0} = -(A+B)} \;. \tag{2.64}$$

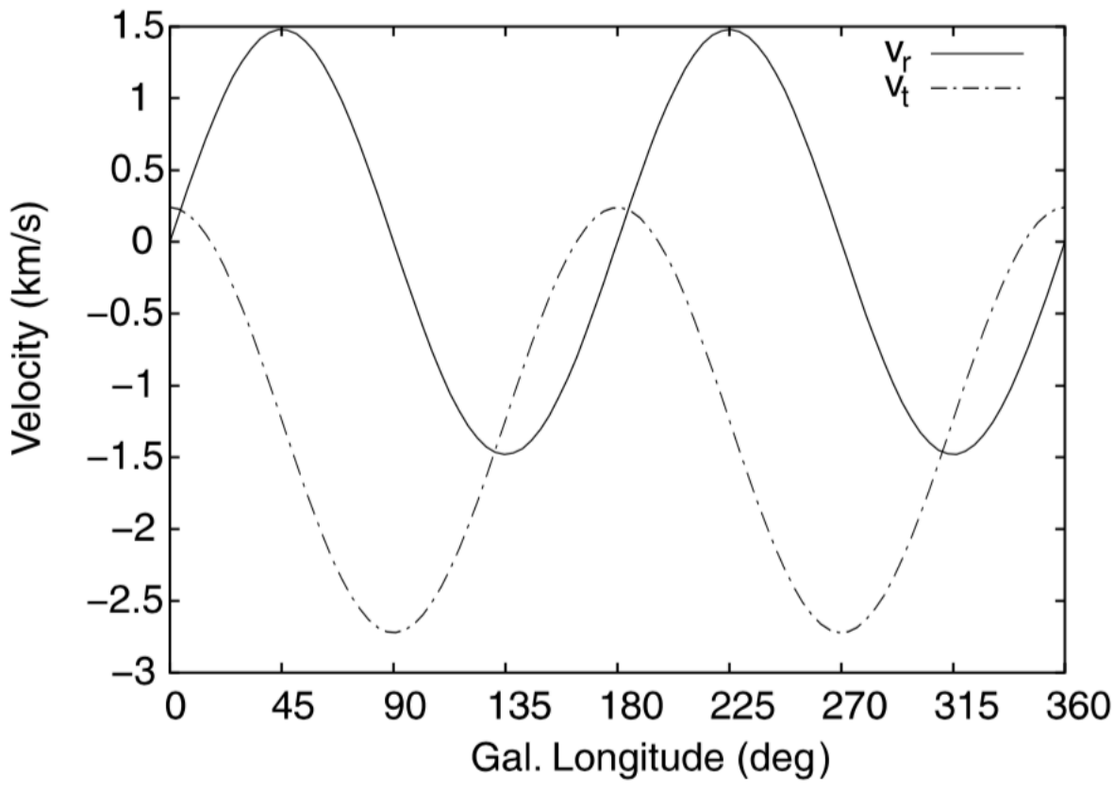

Fig. 2.17. The radial velocity v_r of stars at a fixed distance D is proportional to $\sin 2\ell$; the tangential velocity v_t is a linear function of $\cos 2\ell$. From the amplitude of the oscillating curves and from the mean value of v_t the Oort constants A and B can be derived, respectively (see (2.62))

$$\boxed{\begin{aligned} A &= (14.8 \pm 0.8)\ \mathrm{km\,s^{-1}\,kpc^{-1}} \;, \\ B &= (-12.4 \pm 0.6)\ \mathrm{km\,s^{-1}\,kpc^{-1}} \end{aligned}} \;.$$

Rotation Curve of the Galaxy

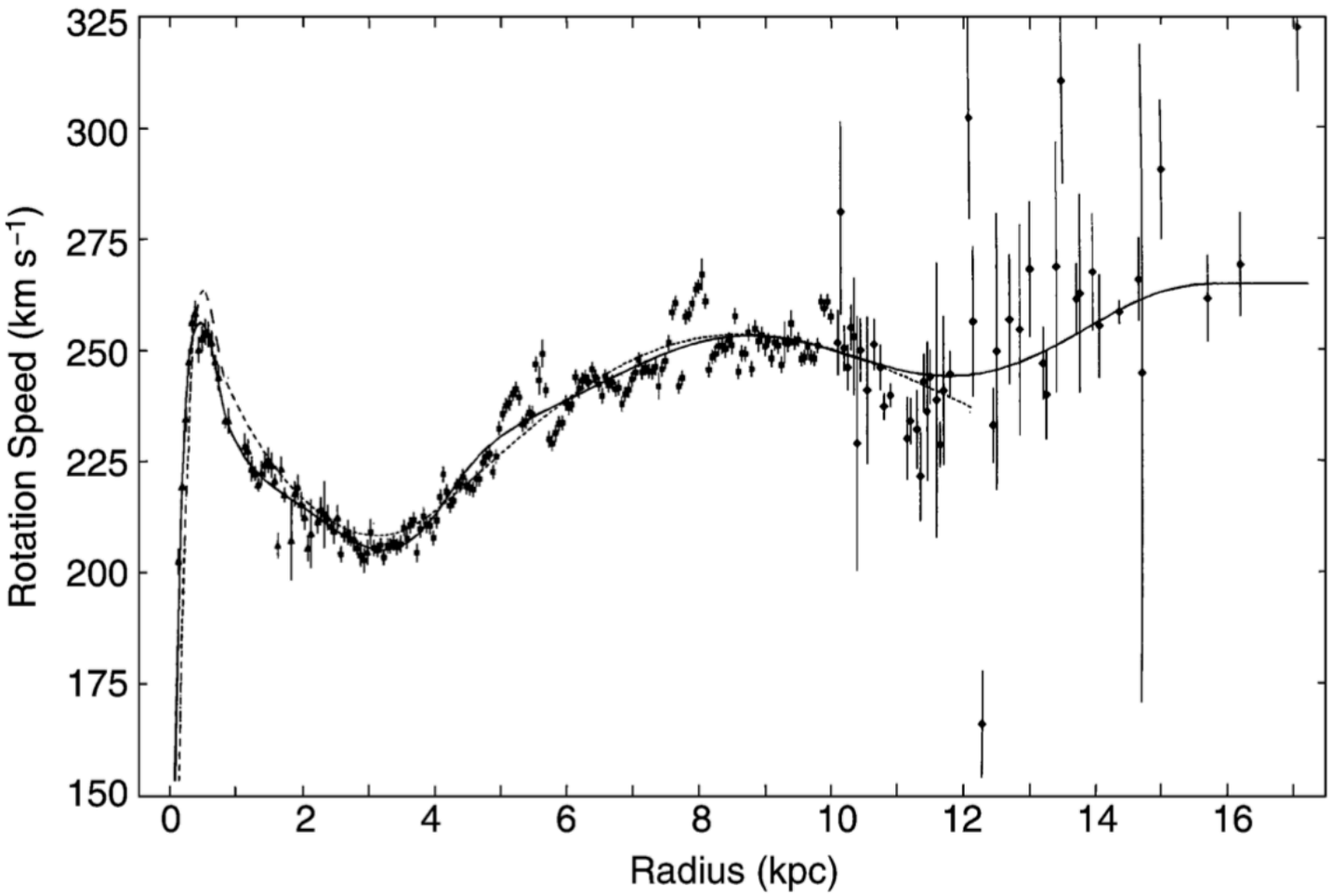

Fig. 2.20. Rotation curve of the Milky Way. Inside the "Solar circle", that is at $R < R_0$, the radial velocity is determined quite accurately using the tangent point method; the measurements outside have larger uncertainties

Dark matter dominates

Stellar Populations

Concept:

A single generation of stars characterized by:

- same age
- same chemical composition
- spacial distribution
- cinematics

=> Several stellar populations coexist in most galaxies

Stellar Populations

The Milky Way:

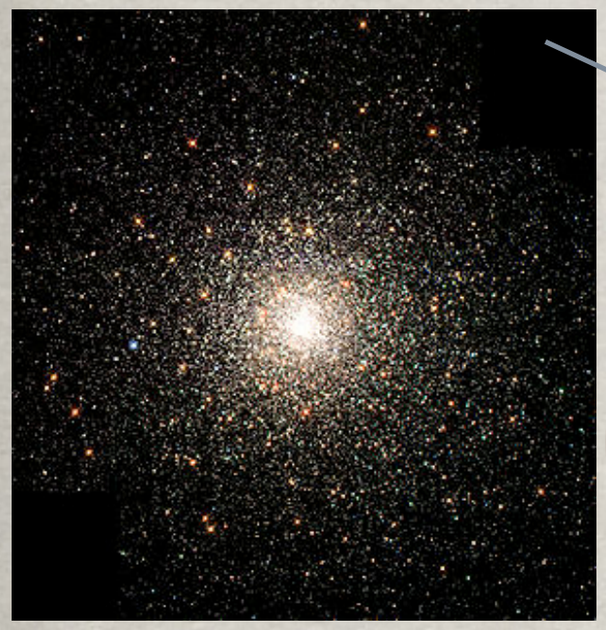

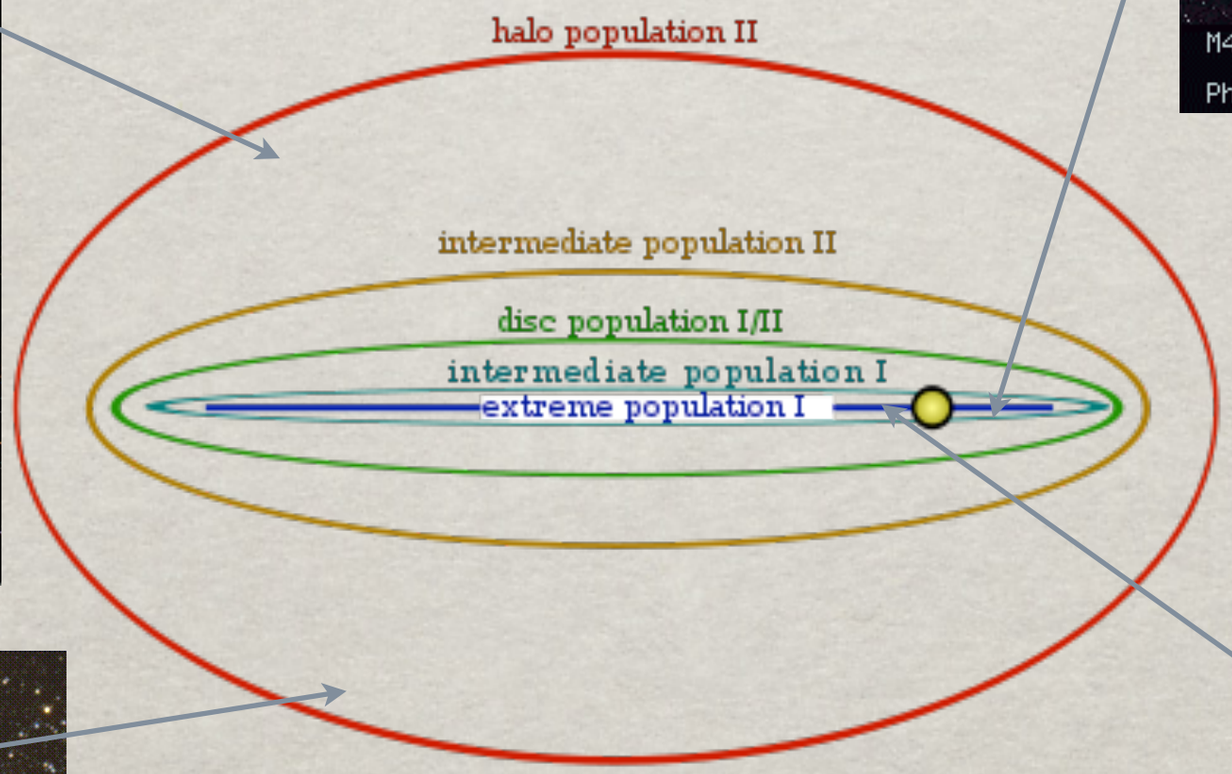

Distribution of Star Populations
in Milky Way

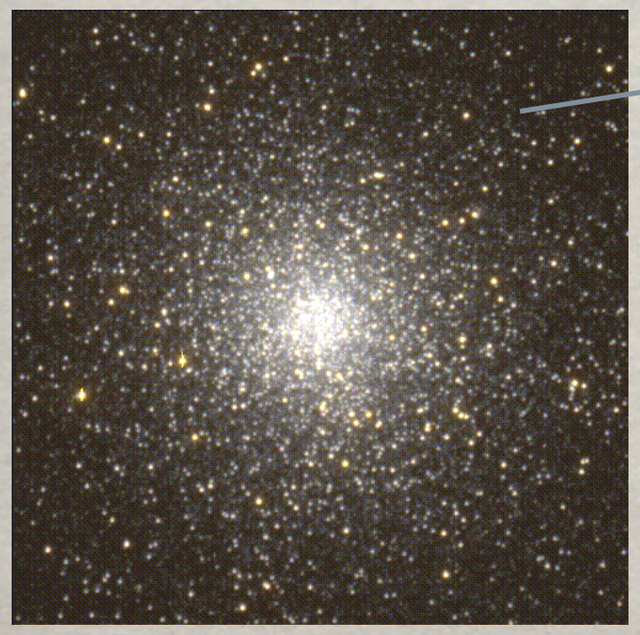

Stellar Populations

The Milky Way:

- Thick and Thin Disks
- Halo and Bulge

Seen in other galaxies as well

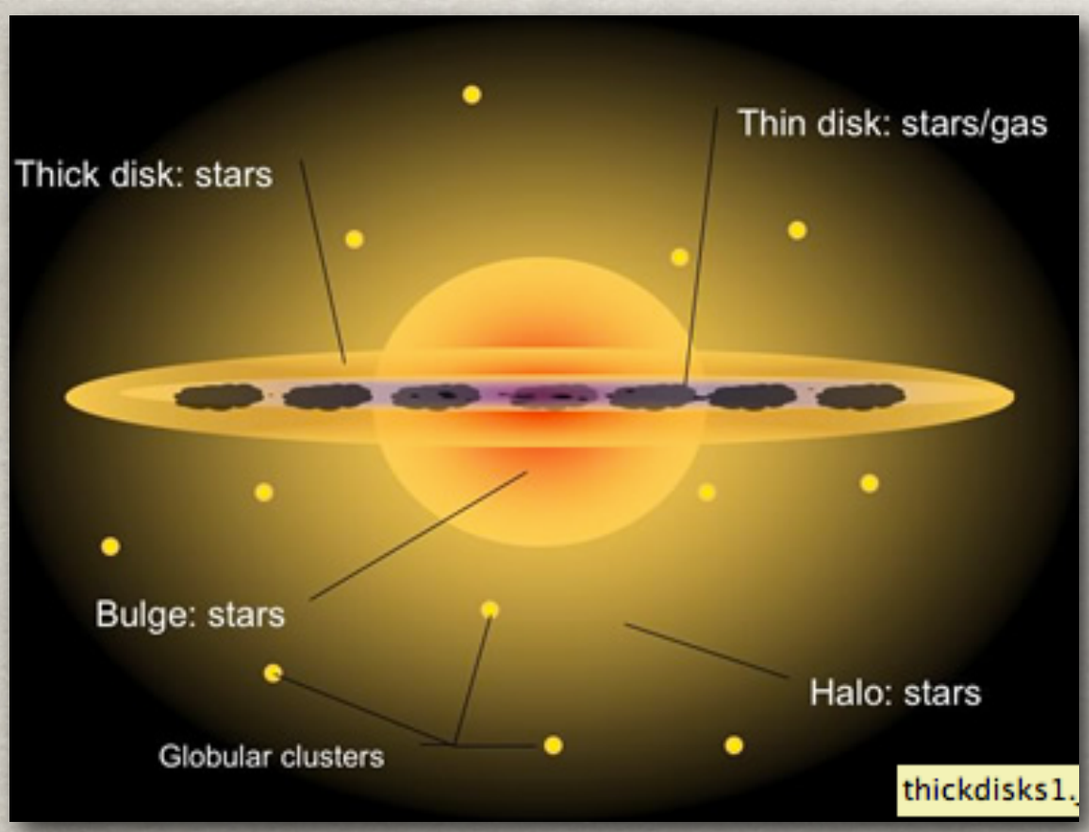

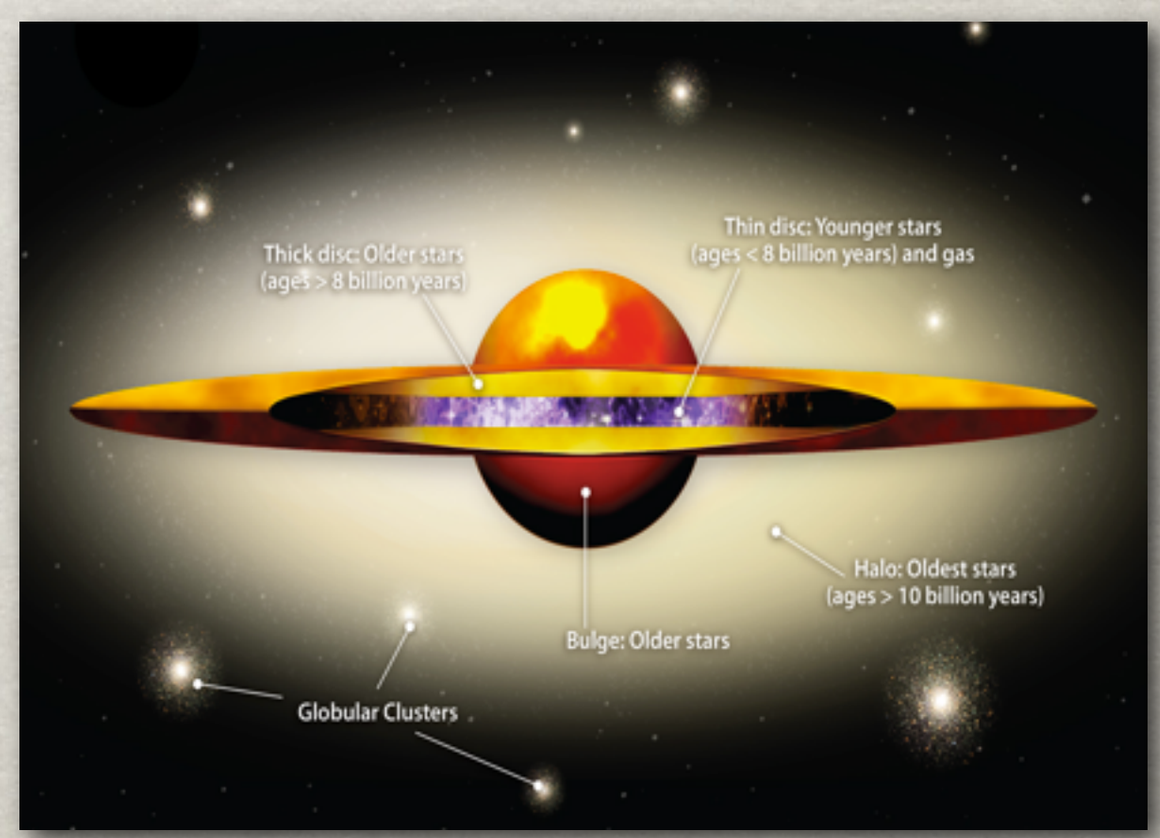

The thick disk is purely stellar in contrast with the thin disk, rich in gas and dust.

Stellar Populations

The Milky Way:

Oldest ---Older----Younger-----Youngest

Halo ----Bulge----Thick Disk---Thin Disk

> 10 Gyr | > 8 Gyr | < 8 Gyr + gas

Halo Population II	Intermediate Pop II Disk Pop I/II Intermediate Pop I
	Extreme Population I

TABLE 3-6. Properties of Stellar Populations

	Population group				
	Extreme Population I	*Older Population* I	*Disk Population* II	*Intermediate Population* II	*Halo Population* II
Typical Objects	Interstellar dust and gas Supergiants T Tauri stars Spiral arms Classical cepheids	Sun Strong-line stars A stars Me dwarfs	Weak-line stars Planetary nebulae Galactic nucleus Novae RR Lyrae stars ($P < 0.4$ day)	High-velocity stars ($Z > 30$ km/sec) Long-period variables ($P < 250$ days)	Globular clusters Extreme metal-poor stars (subdwarfs) RR Lyrae stars ($P > 0.4$ day)
Properties					
$\langle\|z\|\rangle$, pc	120	160	400	700	2000
$\langle\|Z\|\rangle$, km/sec	8	10	17	25	75
Distribution	Extremely patchy	Patchy	Smooth	Smooth	Smooth
Abundance of metals/hydrogen	0.03	0.02	0.01	0.01	0.001
Age (10^9 yr)	<0.1	0.1–1.5	1.5–5	5–6	6
Total mass ($10^9 \mathfrak{M}_\odot$)	2	5	47	47	16
Brightest stars (M_{vis})	−8	−8	−3	−3	−3

Source: Adapted from A. Blaauw, in A. Blaauw and M. Schmidt (eds.), *Galactic Structure*, Chicago: University of Chicago Press, 1965, p. 444, by permission.

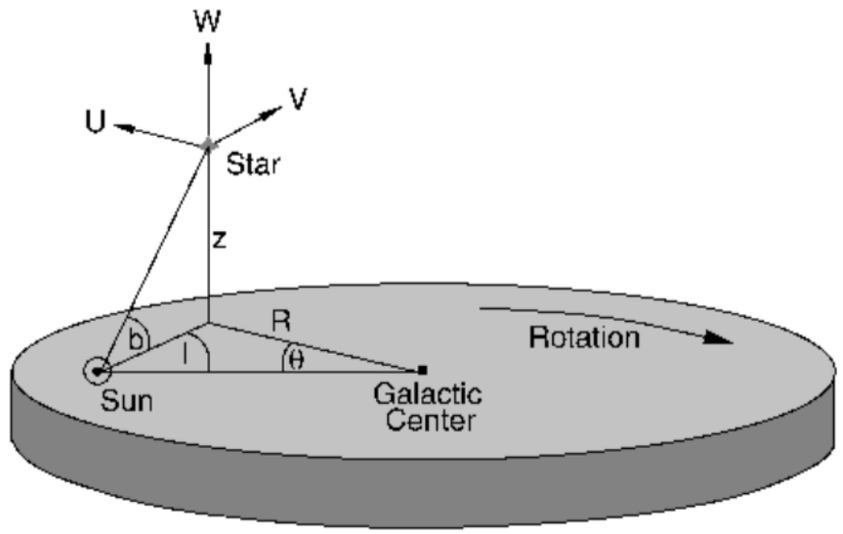

Fig. 2.13. Cylindrical coordinate system (R, θ, z) with the Galactic center at its origin. Note that θ increases in the clockwise direction if the disk is viewed from above. The corresponding velocity components (U, V, W) of a star are indicated

Table 4-18. Archetype Disk-Population Groups

Property	Spiral-arm population	Disk population		
		Young	Intermediate	Oldest
Representative objects	Interstellar gas and dust Open clusters and stellar associations O–B stars Supergiants Classical Cepheids T Tauri stars *Some* stars of type A and later	A stars F stars A–K giants Me dwarfs *Some* G, K, and M dwarfs and white dwarfs	Sun Most G dwarfs *Some* K and M dwarfs and white dwarfs *Some* subgiants and red giants Planetary nebulae	*Some* K and M dwarfs and white dwarfs *Some* subgiants and red giants Moderately metal-poor (weak-lined) stars Long-period variables RR Lyraes, $\Delta S < 5$, $P < 0^d.5$
Age (10^9 years)	$\lesssim 0.1$	~ 1	~ 5	$\lesssim 10$ (?)
$\langle \sigma^2 \rangle^{1/2}$ (km s^{-1})	15	25	50	80
$\langle u^2 \rangle^{1/2}$ (km s^{-1})	10	20	40	60
$\langle v \rangle$ (km s^{-1})	≈ 0	-10	-25	-50
$\langle w^2 \rangle^{1/2}$ (km s^{-1})	10	15	25	40
$\langle \lvert z \rvert \rangle$ (pc)	120	200	400	700
e	0	$\lesssim 0.1$	$\lesssim 0.2$	$\lesssim 0.4$
$(Z/Z_\odot)$	1 to 2	1 to 2	0.5 to 1	0.2 or 0.3 to 0.5
H-R diagram	h and χ Persei	Hyades	M67	NGC 188

Stellar Populations

Tools for its study:

Resolved systems: HR Diagram
CM Diagram

Unresolved systems: Photometry
Spectroscopy
Spectral synthesis

HR Diagram

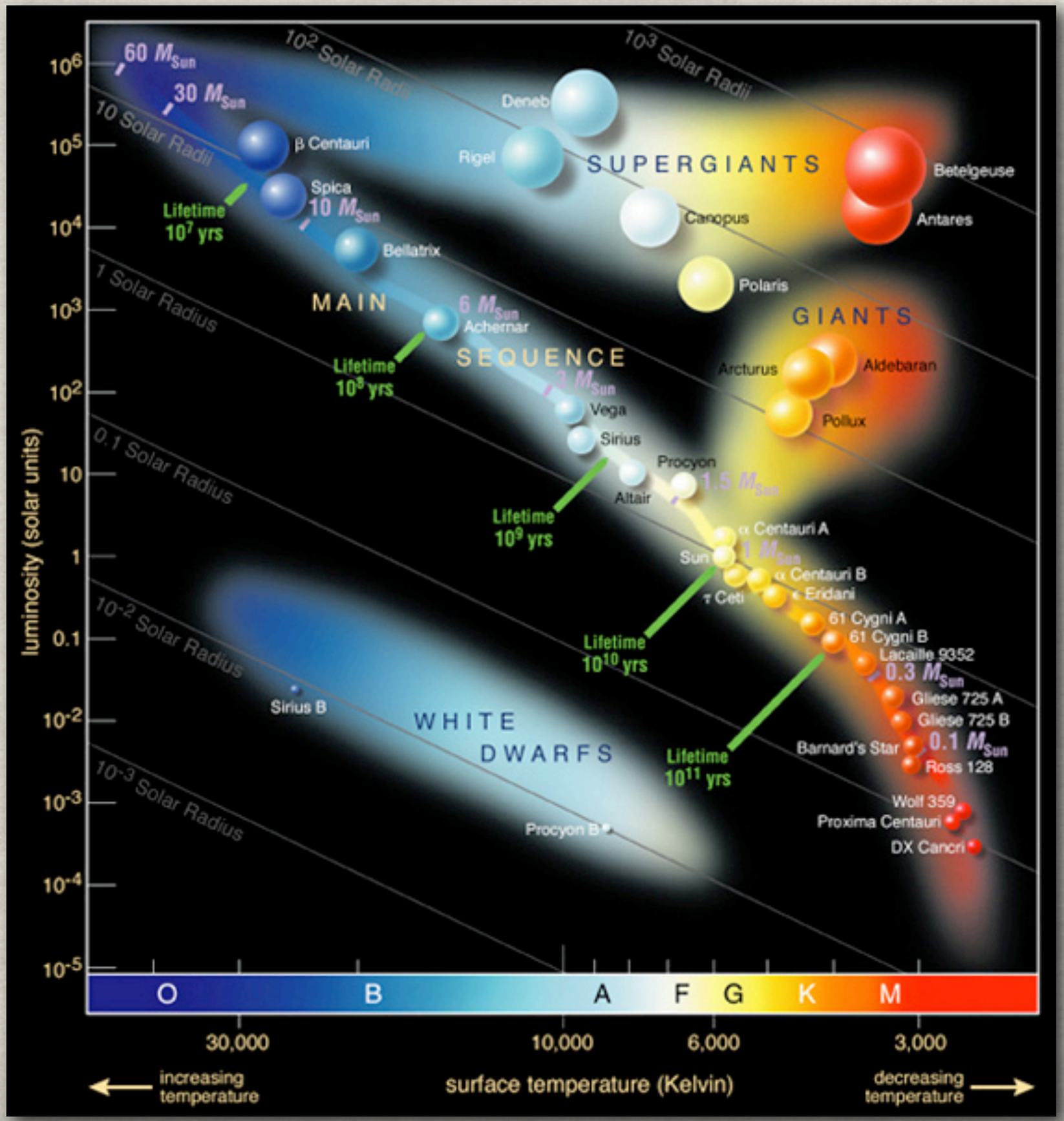
luminosity (solar units)
10^6
10^5
10^4
10^3
10^2
10
1
0.1
10^{-2}
10^{-3}
10^{-4}
10^{-5}
60 M_{Sun}
30 M_{Sun}
10 M_{Sun}
6 M_{Sun}
3 M_{Sun}
1.5 M_{Sun}
1 M_{Sun}
0.3 M_{Sun}
0.1 M_{Sun}
10^2 Solar Radii
10^3 Solar Radii
10 Solar Radii
1 Solar Radius
0.1 Solar Radius
10^{-2} Solar Radius
10^{-3} Solar Radius
Lifetime 10^7 yrs
Lifetime 10^8 yrs
Lifetime 10^9 yrs
Lifetime 10^{10} yrs
Lifetime 10^{11} yrs
Deneb
Rigel
SUPERGIANTS
Betelgeuse
Antares
Canopus
Polaris
β Centauri
Spica
Bellatrix
MAIN
SEQUENCE
Achernar
GIANTS
Arcturus
Aldebaran
Pollux
Vega
Sirius
Procyon
Altair
α Centauri A
Sun
α Centauri B
τ Ceti
ε Eridani
61 Cygni A
61 Cygni B
Lacaille 9352
Gliese 725 A
Gliese 725 B
Barnard's Star
Ross 128
Wolf 359
Proxima Centauri
DX Cancri
Sirius B
Procyon B
WHITE
DWARFS
O
B
A
F
G
K
M
30,000
10,000
6,000
3,000
increasing temperature
surface temperature (Kelvin)
decreasing temperature

CM Diagram

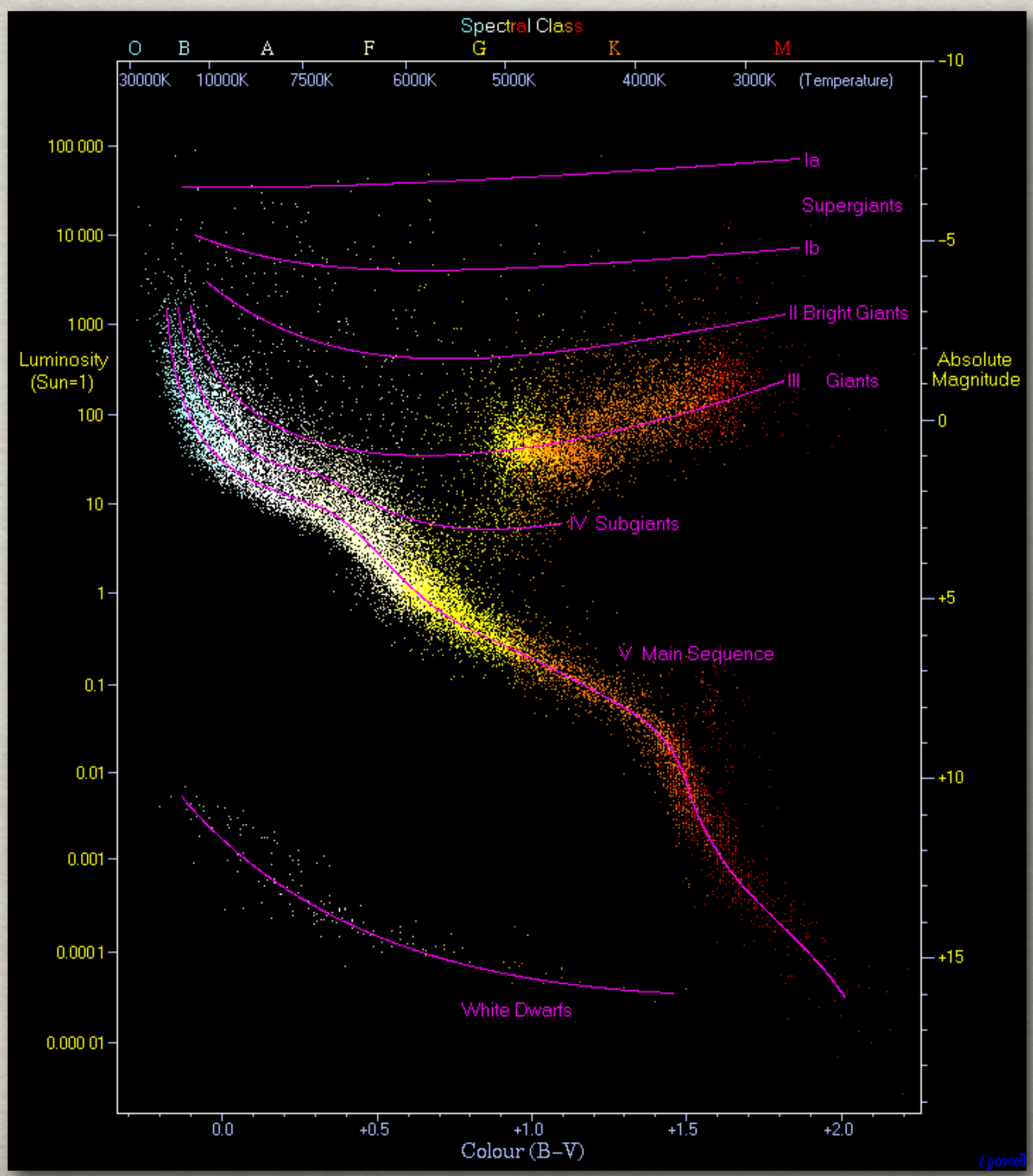
Spectral Class
O
B
A
F
G
K
M
30000K
10000K
7500K
6000K
5000K
4000K
3000K
(Temperature)
100 000
10 000
1000
100
10
1
0.1
0.01
0.001
0.0001
0.000 01
Luminosity
(Sun=1)
-10
-5
0
+5
+10
+15
Absolute
Magnitude
Ia
Supergiants
Ib
II Bright Giants
III Giants
IV Subgiants
V Main Sequence
White Dwarfs
0.0
+0.5
+1.0
+1.5
+2.0
Colour (B–V)
r powell

Stellar Populations in the HRD/CMD

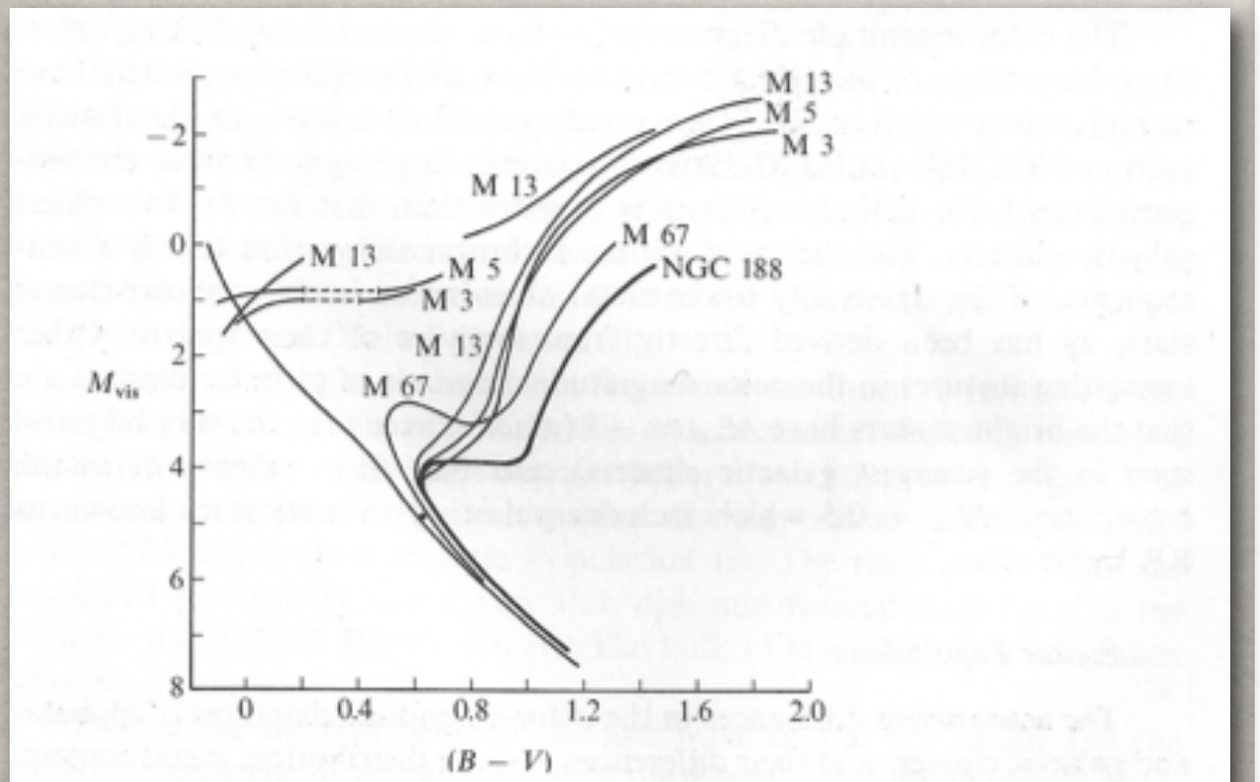

FIG. 3-12. Color-magnitude diagram for the globular clusters M3, M5, and M13, and the old galactic clusters M67 and NGC 188. NGC 188 is the oldest galactic cluster known at present. The difference in the giant branches of the globular and galactic clusters is related to the much lower metal content of globular-cluster stars. (From A. R. Sandage, *Astrophys. J.*, **125,** 333, 1962, by permission.)

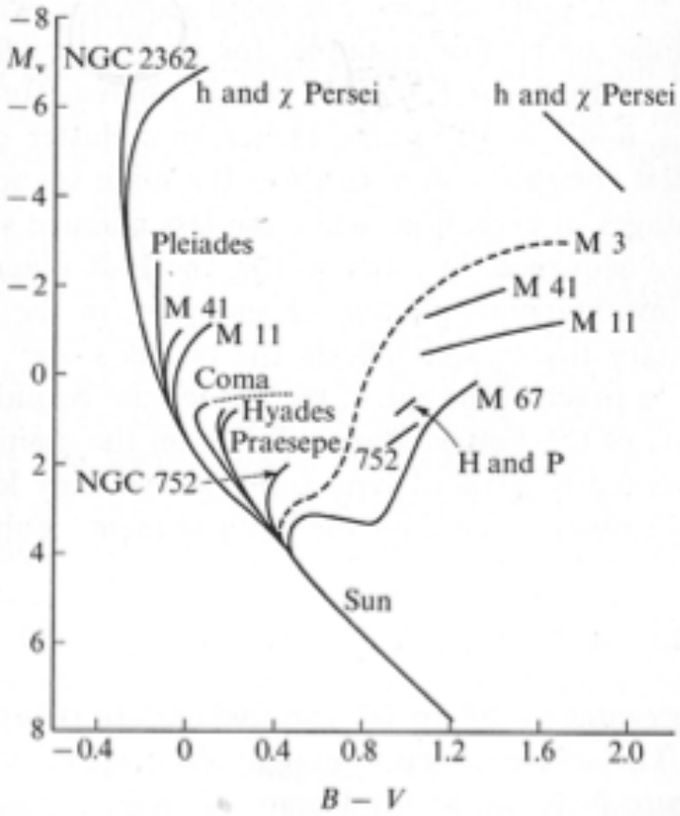

FIG. 3-11. Color-magnitude diagram for several galactic clusters. The cluster M3 is a globular cluster and represents Population II. All other clusters in the diagram are Population I objects. NGC 2362 is the youngest cluster shown, and M67 is the oldest. (From A. R. Sandage, *Astrophys. J.*, **125,** 435, 1957, by permission.)

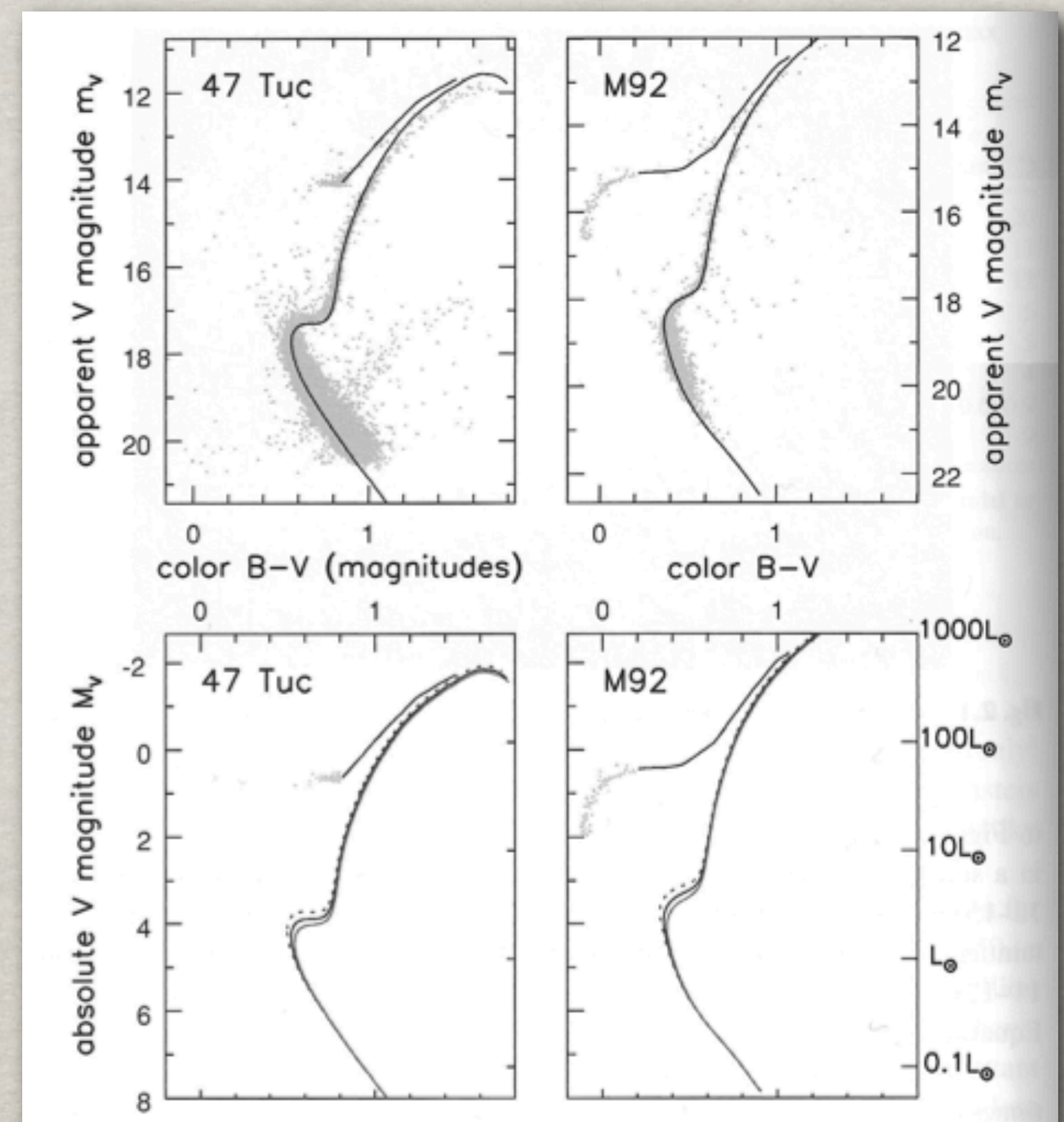

Fig. 2.14. Above, color–magnitude diagrams for globular clusters 47 Tucanae and M92; all vertical scales coincide in luminosity. Above left, the star sequence crossing the main sequence near $B - V, m_V = (0.8, 19.5)$ is the red giant branch of the Small Magellanic Cloud, seen in the background. The model curve shows stars that are 12 Gyr old. Above right, the model curve is for metal-poor stars of age 13 Gyr. Below, the central isochrones match those above; the dotted lines show stars 2 Gyr younger, and the lighter lines those 2 Gyr older – P. Stetson; models from BaSTI at Teramo Observatory.

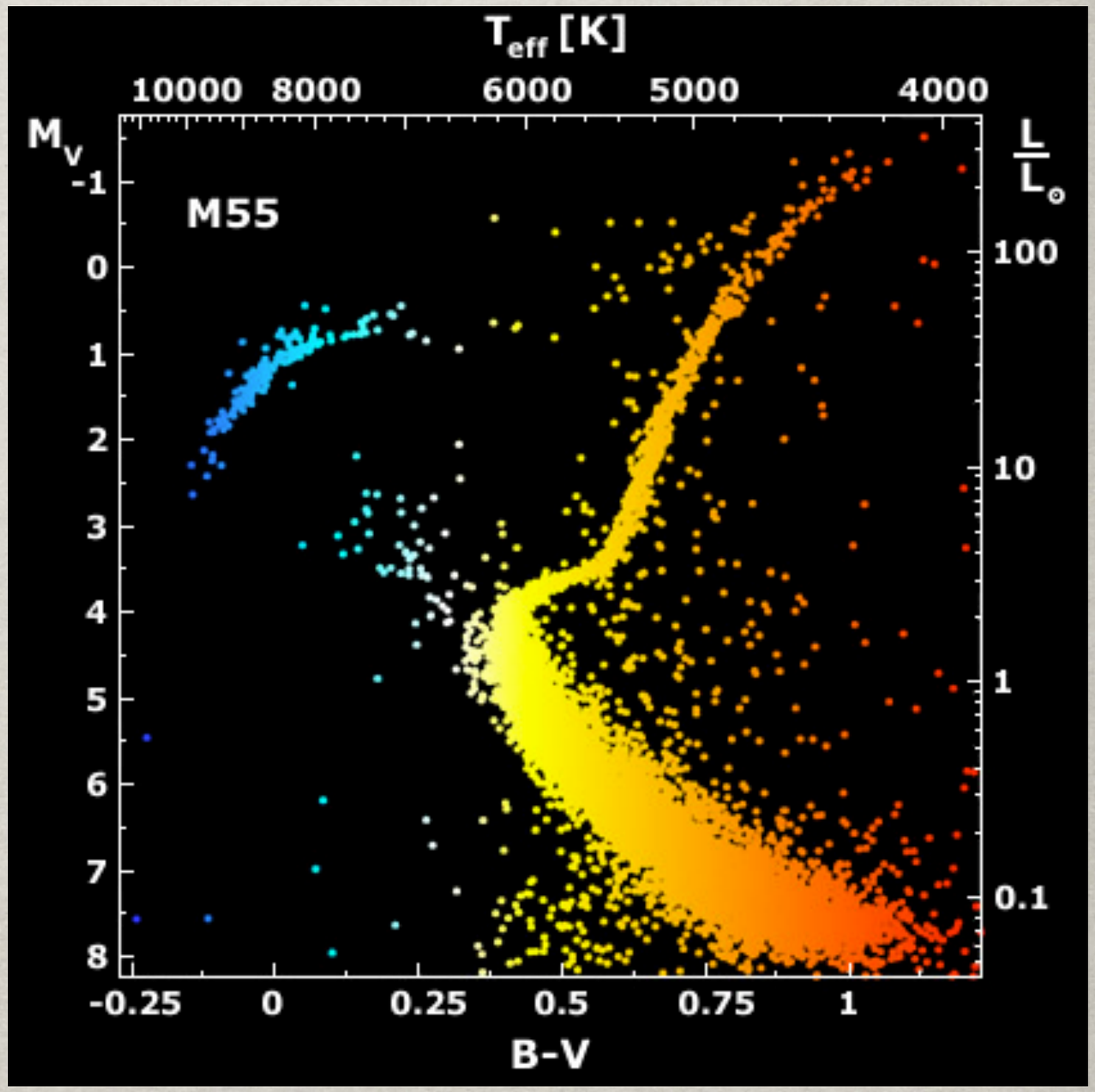
T_eff [K]
10000
8000
6000
5000
4000
M_V
-1
0
1
2
3
4
5
6
7
8
M55
L/L_⊙
100
10
1
0.1
-0.25
0
0.25
0.5
0.75
1
B-V

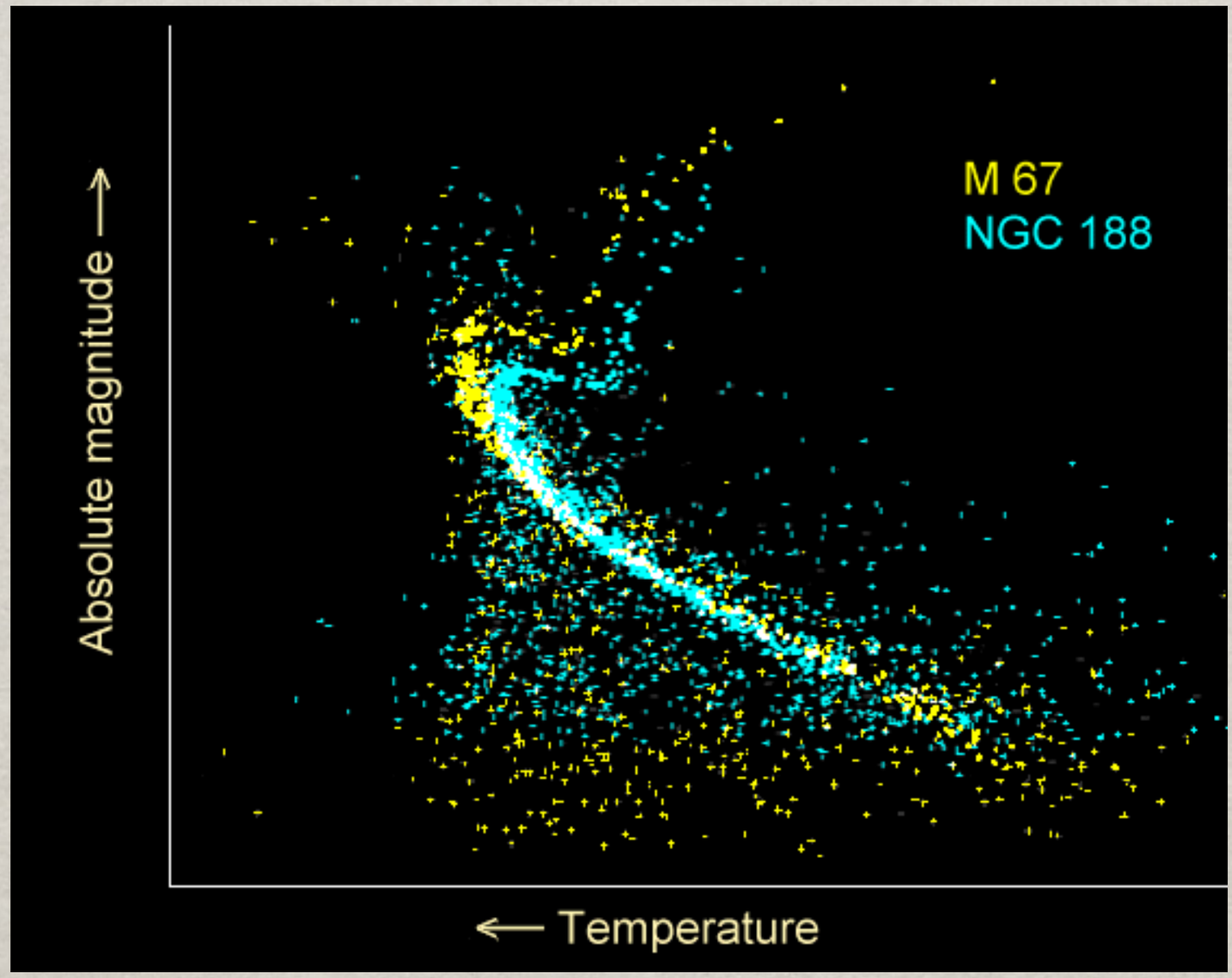
M 67
NGC 188
Absolute magnitude ⟶
⟵ Temperature